Biogeosciences Discuss., https://doi.org/10.5194/bg-2017-410
Manuscript under review for journal Biogeosciences
Discussion started: 13 October 2017


# Methane oxidizing seawater microbial communities from an Arctic shelf

Christiane Uhlig[1]*, John B. Kirkpatrick[2], Steven D´Hondt[1], Brice Loose[1]

[1] Graduate School of Oceanography, University of Rhode Island, Narragansett, RI 02882, USA
[2]The Evergreen State College, Olympia, WA, 98505, USA
*current address: Alfred Wegener Institute Helmholtz Centre for Polar and Marine Research, Bremerhaven, 27570, Germany

*Correspondence to*: Christiane Uhlig (cuhlig@uri.edu)

**Abstract.** Microbial communities of the ocean can consume methane dissolved in seawater before it has a chance to escape to the atmosphere and contribute to greenhouse warming. Seawater over the shallow Arctic shelf is characterized by excess methane compared to the atmospheric equilibrium originating in sediments, permafrost and hydrates. Particularly high concentrations are found beneath sea ice. We studied the structure and methane oxidation potential of the microbial communities from seawater collected close to Utqiagvik, Alaska, in April 2016. The in situ methane concentrations were 16.3 ± 7.2 nmol $L^{-1}$, approximately 4.8 times oversaturated compared to the atmospheric equilibrium. The group of methane oxidizing bacteria (MOB) in the natural seawater and seawater incubations was >97% dominated by Methylococcacales (γ-Proteobacteria). Incubations of seawater under a range of methane concentrations led to a loss of diversity in the bacterial community. The abundance of MOB was low with maximal fractions of 2.5% at 200 times elevated methane concentration, while sequence reads of non-MOB methylotrophs were four times more abundant than MOB in most incubations. The abundances of MOB as well as non-MOB methylotrophs correlated tightly with the rate constant ($k_{ox}$) for methane oxidation, indicating that non-MOB methylotrophs might be coupled to MOB and involved in community methane oxidation. In sea ice, where methane concentrations of 82 ± 35.8 nmol $kg^{-1}$ were found, *Methylobacterium* (α-Proteobacteria) was the dominant MOB with a relative abundance of 80%. MOB abundances were very low in sea ice, with maximal fractions found at the ice-snow interface (0.1%), while non-MOB-methlylotrophs were present in abundances compared to natural seawater communities. The differences in MOB taxa and an offset in methane concentration and stable isotope ratios between the ice and the water column point toward different methane cycling processes in both habitats.

## 1 Introduction

Methane ($CH_4$) is the third most abundant greenhouse gas contributing to climate change (IPCC, 2014) – exceeded only by water vapor and carbon dioxide. Despite much lower concentrations than carbon dioxide it has a 25x higher radiative forcing potential (IPCC, 2014). In the ocean, the two major sources of methane are biogenic production by microbes in anoxic sediments (Formolo, 2010; Reeburgh, 2007; Whiticar, 1999) and release from geological storage (summarized by Kvenvolden and Rogers, 2005; Saunois et al., 2016). Other sources include release from permafrost, river runoff, submarine

groundwater discharge (Lecher et al., 2016; Overduin et al., 2012) and production from methylated substrates under aerobic conditions (Damm et al., 2010; Karl et al., 2008; Repeta et al., 2016). More than 90% of the methane sourced in the seabed is oxidized inside the sediment by anaerobic and aerobic oxidation (Barnes and Goldberg, 1976; Boetius and Wenzhöfer, 2013; Knittel and Boetius, 2009; Reeburgh, 1976). The remaining fraction of methane either diffuses into the water at the sediment surface, or can be released as bubbles, which completely or partially dissolve while rising through the water column (Leifer and Patro, 2002). Dissolved methane is used as a substrate and oxidized by aerobic methanotrophic bacteria (methane oxidizing bacteria, MOB) in the water column (Hanson and Hanson, 1996; Murrell, 2010). As a result of these biological processes oceanic methane concentrations are frequently found at low nanomolar levels, leaving only a small fraction of subseafloor sourced methane to eventually exchange with the atmosphere (Karl et al., 2008; Reeburgh, 2007).

By contrast, in the Subarctic and Arctic shelf areas, shallow water depths and seasonal sea ice cover complicate the picture. High concentrations of methane have been reported from the entire water column up to the surface around Svalbard (Damm et al., 2005; Mau et al., 2013), the Siberian Shelf (Shakhova et al., 2010) and the Beaufort Sea (Lorenson et al., 2016). In addition, during periods of near 100% sea ice cover, gas exchange from the water column to the atmosphere is restricted (Loose et al., 2011). While under ice free conditions methane concentrations are frequently found in the range of 15 to 30 nmol $L^{-1}$ or around 700% supersaturated with regard to the atmospheric equilibrium, winter concentrations are often 10 to 100 times higher. Maximal concentrations of 5000 nmol $L^{-1}$, or an oversaturation of 160000%, have been reported from the Siberian Shelf (Lorenson et al., 2016; Shakhova et al., 2010; Zhou et al., 2014).

Besides others factors like oxygen and trace metal availability (Crespo-Medina et al., 2014; Sansone et al., 2001; Semrau et al., 2010), dissolved methane concentration is an important control on the community of MOB and thus methane oxidation rates (Crespo-Medina et al., 2014; Kessler et al., 2011; Mau et al., 2013). Methane hotspots, promoted by limited gas exchange under sea ice, might thus be candidate regions for accumulation of methane oxidizers. In addition, sea ice and in particular the ice water interface is a hotspot for microbial activity. The ice surface, penetration of light and the constant exchange with the underlying water column favor the development communities composed of small eukaryotic organisms, microalgae, prokaryotes and viruses; the biomass often being several orders of magnitudes denser than in the underlying water column (Thomas and Dieckmann, 2002).

Methane oxidizing bacteria use methane as their sole carbon and energy source (Hanson and Hanson, 1996). In the first step methane is oxidized to methanol catalyzed by the enzyme methane mono-oxygenase. Since methane mono-oxygenase is characteristic to nearly all MOB (Knief, 2015), *pmoA*, the gene encoding for a subunit of the membrane bound particulate methane mono-oxygenase, has been used as specific molecular marker for detection and characterization of MOB (Knief, 2015; Lüke and Frenzel, 2011; reviewed by McDonald et al., 2008). Methanol is further metabolized to formaldehyde, from where it is either mineralized to carbon dioxide ($CO_2$), or assimilated into organic carbon compounds and finally biomass (reviewed by Hanson and Hanson, 1996; reviewed by Strong et al., 2015). Different types of MOB are distinguished by their phylogeny and assimilation pathway for formaldehyde. While γ-Proteobacteria or Type I MOB assimilate formaldehyde via the ribulose monophosphate pathway (RuMP), α-Proteobacteria or Type II MOB use the serine pathway (Hanson and

Hanson, 1996). Besides these two proteobacterial groups, MOB were recently also identified in the phylum Verrucomicrobia (e.g. Dunfield et al., 2007; Pol et al., 2007).

Methane-derived carbon has further been shown to be assimilated in methylotrophic or other bacteria in freshwater and temperate marine environments. This is attributed to cross feeding by non-methane oxidizers on metabolites produced by the MOB (Hutchens et al., 2003; Jensen et al., 2008; Saidi-Mehrabad et al., 2013).

Knowledge of the microbial communities responsible for methane oxidation in the Arctic and Subarctic is still sparse. During the last years the first few studies have determined methane oxidation rates from seawater in these regions to cover a range from $10^{-4}$ up to 3.2 nmol $L^{-1}$ $d^{-1}$ (Gentz et al., 2014; Lorenson et al., 2016; Mau et al., 2013, 2017; Steinle et al., 2015). In only two of these studies, both performed off Svalbard, oxidation rate measurements were combined with analysis of the microbial community. Steinle et al. (2015) quantified MOB by fluorescence in situ hybridization and microscopy. Low but relatively constant cell specific oxidation rates were determined from the oxidation rates and MOB abundance, indicating that MOB community size is an important control on the total methane oxidation rate in the system. Mau et al. (2013) analyzed the bacterial community with denaturing gradient gel electrophoresis (DGGE) of the 16S gene and compared patterns of PCR products for *pmoA*. Different MOB communities were observed in the meltwater layer and deep water in this stratified system, also reflecting the observed differences in methane oxidation rates. Only one of the eleven analyzed DGGE bands was identified as methanotroph from the genus *Methylosphaera* from the deep water in this study, while none were detected in the meltwater, possibly due to the limitations of the method. To our knowledge, no high-throughput sequencing studies of methane oxidizing bacteria in the Arctic have been published in peer-reviewed literature to date.

We studied methane oxidizing communities from seawater sampled on the Beaufort Sea shelf close to Utqiagvik, Alaska. Incubation experiments were performed under different methane concentrations to directly compare the bacterial community structure with methane oxidation rates. Seawater incubations as well as freshly sampled sea water and sea ice were analyzed for their entire community diversity (16S rDNA) and the presence of MOB (16S rDNA and *pmoA*) using high-throughput Illumina MiSeq sequencing. The aim of this study was to (1) investigate the response of the entire microbial community to an increase in methane abundance, (2) identify types of MOB involved in the oxidation of methane, (3) test for the presence of MOB in natural seawater and sea ice communities and (4) relate these community features to methane oxidation rates.

## 2 Methods

### 2.1 Study site

Samples were collected at two sites between 7 April 2016 and 15 April 2016 in the Beaufort Sea (Table 1). Site “Elson Lagoon” (EL) was located north of Utqiagvik, Alaska, (7.4.2016, 71.334° N, -156.363° W), covered with 1.5 m thick sea ice, at approx. 1.5 m water depth, leaving only a narrow layer of water between the sea ice and the sediment. Site “Ice Mass Balance Buoy” (IMB) was located 1 km offshore of Utqiagvik, close to the ice mass balance buoy of the sea ice physics

group of University of Alaska, Fairbanks (7.4.2016, 71.373° N, -156.548° W, and 9.4.2016, 71.372° N, -156.540° W). This site was characterized by 1 m thick fast ice cover and a water depth of approximately 7 m.

### 2.2 Sampling and instrument deployment

Seawater temperature and salinity records were taken with an YSI Professional Plus probe (YSI, Ohio, USA) and a YSI 600 OMS V2 sonde. Water was collected using either a peristaltic pump (Masterflex Environmental Sampler, Cole Parmer, Illinois, USA) or submersible pump (Cyclone, Proactive Environmental Products, Florida, USA). For determination of methane concentration and isotope ratios, water samples were collected as described in Uhlig and Loose (2017). Briefly, in the field 0.7-0.9 L seawater was transferred bubble free directly into in foil sample bags (# 22950, Restek, Pennsylvania, USA). Upon return to the laboratory, a 0.1 L headspace of Ultra-High Purity nitrogen (Air Liquide, Anchorage, AK) was introduced into the bags through the septa, and the samples were equilibrated at 30°C for in situ measurements for at least 6 h.

For DNA extractions between 1–2 L of seawater were filtered onto Sterivex® filter cartridges (Millipore) with 0.2 µM PES filter membranes directly in the field, or were filled into foldable polypropylene containers and filtered upon return to the laboratory. For nutrient analysis an aliquot of the flow through of the Sterivex® filters was collected in 15 mL polypropylene tubes (Falcon Brand, Corning, New York, USA) and frozen at -80°C. Seawater was fixed with 2% final concentration formaldehyde (Mallinckrodt Chemicals, Surrey, UK) and stored at 5°C to for later determination of the cell number.

Additionally, at site IMB seawater temperature, salinity and velocities were recorded with an Aquadopp Profiler (Nortek AS, Norway), and a salinity temperature recorder (SBE37SMP, Sea-Bird Scientific, Washington, USA). These were deployed at about 7 m depth on the seafloor between 9 and 15 April.

Sea ice was collected at site IMB only, using a Kovacs Mark II ice corer (Kovacs, Roseburg, Oregon, USA). The ice cores were sectioned into 15 cm, split lengthwise and the outside was cleaned with a sterilized knife to remove microbes possibly transferred from the sampling equipment. The core sections were sealed into custom made gas tight tubes (Loose et al., 2011) for determination of methane concentration and isotope ratios. In the laboratory the gas tight tubes were flushed with ultrapure nitrogen for several gas volumes (Lorenson and Kvenvolden, 1995). The ice samples were melted at room temperature, with frequent mixing within a day (IC2), or within a week at 5°C (IC1). Samples for molecular biology and cell counts were collected from the melted sea ice similar to the procedure described for seawater. In addition, the bottom 2 cm of one ice core was sampled into a sterile sample bag (Whirlpak, Nasco, Fort Atkinson, WI, USA) for molecular biology processing only. Sea ice brine volume fractions were calculated according to Cox and Weeks (1983).

### 2.3 Oxidation rates and determination of isotope fractionation factors

Methane oxidation rates were determined from the methane mass balance according to Uhlig and Loose (2017). In short, seawater was sampled into multi-layer foil bags. In addition to a headspace of hydrocarbon-free air (Air Liquide, Anchorage,

AK), the sampling bags were supplied with a spike of methane. Final methane concentrations ranged between 3.0 and 4000 nmol $L^{-1}$ representing approximately 0.2x (without methane addition), 2x, 10x and 200x of the in situ methane concentration. Samples were incubated at 0-1°C for 5 to 46 days. Assuming first order kinetics for the oxidation of methane (Reeburgh et al., 1991; Valentine et al., 2001), oxidation rate constants ($k_{ox}$) were determined from the methane mass balance in the incubations (Uhlig and Loose, 2017) as

$$\ln\left(\frac{n(CH_4)_{total,\ t_i}}{n(CH_4)_{total,\ t_{i-1}}}\right) = -k_{ox,ppm} \times\ t_{i-(i-1)} \quad (1)$$

with $n(CH_4)_{total,\ t_i}$ being the total molar mass of methane in the bag at time $t_i$.

The oxidation rate ($r_{ox}$) was calculated from the first order constant and the in situ concentration of methane in the water:

$$r_{ox} = k_{ox} \times c(CH_4)_{w,\ in\ situ} \quad (2)$$

Isotopic fractionation factors of methane oxidation ($\alpha_{ox} = \frac{k_{12}}{k_{13}}$) were determined as described in (Preuss et al., 2013), using the isotope fractionation approach (Coleman et al., 1981).

$$\ln\left(\frac{c(CH_{4ti})}{c(CH_{4t0})}\right)\left(\frac{1}{\alpha_{ox}} - 1\right) = \ln\left(\frac{1000 + \delta^{13}CH_{4ti}}{1000 + \delta^{13}CH_{4t0}}\right) \quad (3)$$

where the isotope ratios are described in $\delta$-notation $\delta^{13}C = \frac{R_{sample}}{R_{standard}} - 1$, and R is the isotope ratio of $^{13}CH_4/^{12}CH_4$ in the sample and standard (VPDB, Vienna Peedee Belemnite, McKinney et al., 1950), respectively.

Alpha can be determined as $\alpha_{ox} = \frac{1}{m+1}$ from the slope (m) of the linear regression between $ln\left(\frac{c(CH_{4ti})}{c(CH_{4t0})}\right)$ and $\ln\left(\frac{1000 + \delta^{13}CH_{4ti}}{1000 + \delta^{13}CH_{4t0}}\right)$.

### 2.3 Analytical procedures

#### 2.3.1 Methane concentration and stable isotope ratios

Methane concentrations and stable isotope ratios were determined with a Picarro G2201-*i* cavity ring-down spectrometer (Picarro, Santa Clara, California, USA) coupled to a Small Sample Isotope Module (SSIM) as described by Uhlig and Loose (2017). After equilibration, the headspace above the seawater or melted ice was subsampled with a gas tight syringe and 1 to 15 mL injected into the SSIM. Measurements were performed in fast measurement mode. Dissolved methane concentrations were calculated as described in Magen et al. (2014) with the equilibrium constant according to Yamamoto et al. (1976).

#### 2.3.2 Nutrient analysis and flow cytometry

Phosphate, nitrate and nitrite concentrations were determined on a QuickChem QC8500 automated ion analyzer (Lachat, Loveland, Colorado, USA). The total number of prokaryotic cells was counted on a BD Influx™ flow cytometer with BD FACS™ software. Formol fixed samples were stained with a final concentration of 1x SYBR Green I (Invitrogen, Molecular Probes, Eugene, Oregon, USA) for 20 to 45 min at room temperature in the dark before analysis.

### 2.4 Nucleic acid extraction and sequencing

DNA was extracted with the PowerWater® DNA extraction kit (MoBio, Carlsbad, California, USA). To remove the filter membrane, the Sterivex® cartridge was opened with a pair of sterilized pliers. The filter membrane was cut out along the edge with a scalpel, transferred into the bead tube, and DNA subsequently extracted according to the manufacturer's protocol. A minor modification was made: the tube was vortexed two times for 3 minutes and rotated 180° in between. The DNA was eluted in 80 µL buffer PW6, after incubating the buffer for 1 min on the membrane. Quantification was conducted with a Qubit®2.0 Fluorometer (Invitrogen, Carlsbad, California, USA).

The V4V5 region of the 16S rRNA gene was amplified with forward primer 518F (5´-xx-CCAGCAGCYGCGGTAAN-3´), and an 8:1:1 mix of the reverse primers 926R1 (5´-yy-CCGTCAATTCNTTTRAGT-3´), R2 (5´-yy-CCGTCAATTTCTTTGAGT-3´) and R3 (5´-yy-CCGTCTATTCCTTTGANT-3´) (Nelson et al., 2014). Primers included 33 base pair (bp) adapters (xx, yy) at the 5´end. The final volume of 20 µL PCR reaction contained 0.2 µL PfuUltra II fusion HS DNA polymerase (Agilent Technologies, Santa Clara, California, USA), 50 µM each forward and reverse primer, 25 µM each dNTPs (Thermo Scientific, Waltham, Massachusetts, USA), 10 µg $mL^{-1}$ BSA (Thermo Scientific, Waltham, Massachusetts, USA) and 1 ng template DNA. After initial denaturation for 2 min at 95°C, DNA was amplified in 30 cycles of 30 seconds 95°C denaturation, 30 seconds 55°C annealing and 30 seconds at 72°C for extension, with a final extension of 2 minutes at 72°C. The *pmoA* subunit of the particulate monooxygenase (pMMO) was amplified with primer pair 189f (5´-xx-GGNGACTGGGACTTCTGG-3´) and mb661r (5´-yy-CCGGMGCAACGTCYTTACC-3´) (Holmes et al., 1999; Lyew and Guiot, 2003). The PCR conditions were the same as described for the V4V5 amplicon. All amplicons were purified with Agencourt® AMPure® XP magnetic beads (BeckmanCoulter, Indianapolis, Indiana, USA) at a ratio of 0.7x bead solution per PCR reaction volume and washed with 80% ethanol.

The primer sequences specified above included adapter sequences (xx, yy) to attach Nextera indices and adapters in a second PCR reaction of 6 cycles with 50 ng template DNA (http://web.uri.edu/gsc/next-generation-sequencing/). Amplicons were sequenced with Illumina MiSeq at 2x250 bp read length.

### 2.5 Sequence analysis

#### 2.5.1 V4V5

Demultiplexing and adapter removal was performed with Illumina software. V4V5 sequence quality control and clustering was performed in mothur (Schloss et al., 2009) as follows. Contigs were prepared from forward and reverse reads and culled if containing ambiguous bases or homopolymers longer than 6 bases. Sequences observed in kit and filter blanks were removed from all samples. After alignment to the Silva small subunit reference database (v123; Quast et al., 2013), the 408 bp long sequences were preclustered (1% variability allowed) and filtered for chimeras (de novo algorithm) with the UCHIME (Edgar et al., 2011) wrapper in mothur. Sequences identified as Chloroplast, Mitochondria, Archaea, Eukaryota or

unknown were removed and OTUs built at a 3% distance level with the opticlust algorithm. OTUs with fewer than 2 reads were removed from further analysis.

Visualization and further analysis of sequencing data was performed in R version 3.2.3 (R CoreTeam, 2015) in RStudio Version 0.99.903. Species diversity was analyzed using the phyloseq package (McMurdie and Holmes, 2013) testing for the richness (Shannon and Simpson indices) and differences in community structures (Bray-Curtis dissimilarities). Differences of the community structure between different methane spike concentrations were determined via analysis of similarity (ANOSIM) in the package vegan (Oksanen et al., 2017) on three predefined groups: in situ (N=9), 0.2x (N=2) and 10x (N=3). Groups 1x, 200x short, 200x long with N=1 (Table 2), were excluded from the analysis.

### 2.5.2 Identifying potential methane oxidizing bacteria

To select groups representing methylotrophs and methanotrophs, OTUs were filtered according to their phylogenetic annotation assigned by mothur for containing the string "meth" on family, order and genus level. This filter is expected to find 97% of taxonomically annotated methanotrophs according to a current review on the diversity of methanotrophs (Knief, 2015).

Further, phylogenetic groups potentially involved into methane cycling were identified as differentially more abundant OTUs between and spiked treatments (0.2x, 10x, 200x) and in situ samples using DESeq2 (Love et al., 2014). Only OTUs with an adjusted p-value in DESeq2 < 0.05 were kept for further analysis. OTUs identified from spike 0.2x were considered to represent groups favored due to the incubations (the "bottle effect") rather than addition of methane, and removed from further analysis. Treatment IMB 2x, EL 0.2x and EL 10x (Table 2) were not included into the analysis, since no replicate samples were available. The abundance of all candidate OTUs, identified as described above, was determined within every in situ or spiked sample.

Absolute numbers of methanotrophs and methylotrophs were calculated by multiplying the relative 16S sequence abundance with flow cytometric cell counts. The absolute numbers were further corrected for the mean of the 16S gene copy number for the lowest taxonomic rank (class to genus) available in the rrnDB-database (Stoddard et al., 2015).

### 2.5.3 Particulate methane monooxygenase: *pmoA*

In addition to 16S genes, the alpha subunit of the particulate methane monooxygenase (*pmoA*) was used as molecular marker for MOB. Only forward reads were analyzed for *pmoA*. High quality reads were retrieved according to the following protocol. Using mothur (Schloss et al., 2009) all reads were trimmed to a length of 225 bp to remove sequence fractions with a mean quality score below 30 (fastqc; Andrews, 2010). In addition, reads were clipped whenever the average quality score over a 50 bp window dropped below 30. Sequences with ambiguous bases and homopolymers larger than 6 bp were culled. Only sequences that translated into uninterrupted protein reading frames (Emboss 6.60 / transseq; Rice et al., 2000), were kept for further analysis. Nucleic acid sequences were aligned to a reference dataset of *pmoA* sequences (fungene; Fish et al., 2013) and sequences of a length of at least 220 bp were preclustered (1% variability allowed). De novo chimera filtration

was run with the UCHIME (Edgar et al., 2011) wrapper in mothur. A similarity of 93% between *pmoA* sequences was defined to match the 97% cutoff as species definition on the 16S gene (Lüke and Frenzel, 2011). OTUs were built at a maximal distance of 7% between the furthest neighbors, to maximize resolution between OTUs, due to the short read length and limited number of unique sequences (Supplementary Table 1). To determine the phylogenetic relationship of *pmoA* sequences, nucleotide sequences were aligned against selected reference sequences in Mafft 7.017 (Katoh and Standley, 2013) and a neighbor joining tree calculated in Clustal 2.1 (Larkin et al., 2007) with 1000 replications.

## 3 Results

### 3.1 Water column properties

During the sampling in April 2016 the water column at station IMB was characterized by a northeastward directed Barrow Current, with water temperatures around -1.8°C and salinities of 33.9 to 36.4 (Figure 1, Supplementary Figure 1, 2) for most days. Between 11 April and 13 April the current changed southward bringing warmer water (max. temperature observed -0.9°C), reflected in the temperature profile for 11 April. A lower salinity of 27.5 at the ice water interface indicates melting of the sea ice. Phosphate concentrations were 0.99 ± 0.33 µM (N=9) and nitrate 6.59 ± 4.04 µM (N=9), with neither showing any trends in the depth profiles (data not shown). Nitrite concentrations were below detection (0.3 µM based on technical replicates).

Water column methane concentrations at station IMB ranged between 9.2 and 25.3 nmol $L^{-1}$ (16.3 ± 7.2, N=5) (Figure 1), with stable isotope signatures between -55.4 and -70.5 ‰ (-60.6 ± 6.3, N=5)). Total prokaryotic cell densities, determined as SYBR Green stained cells with flow cytometry, were 6.9 x 104 ± 5.7 x 103 cells $mL^{-1}$ (N=16).

The narrow layer of water between the sediment and ice in Elson Lagoon (N=1) had a salinity of 21 and a temperature at the seawater freezing point. Phosphate and nitrate concentrations were 0.74 µM and 4.87 µM, respectively. Methane concentration for Elson Lagoon (N=1) was 53.2 nmol $L^{-1}$ with a stable isotope ratio of -73.8 ‰ (Figure 1) and cell density 7.7 x 104 cells $mL^{-1}$.

### 3.2 Ice cores

Temperature and salinity profiles of the two sea ice cores sampled at 9 and 15 April are shown in Figure 2. Brine volume fractions above 5% indicate that the ice was permeable for water and gases (Golden et al., 1998) in the bottom 50–100 cm, while the upper part of the ice was impermeable. Methane concentrations in the ice were higher than in the water (83.9 nmol $kg^{-1}$ ± 35.0 nmol $kg^{-1}$, N=9) while the isotope signatures were close to seawater (-60.4‰ ± 3.5‰, N=9). Ice core 1 (IC1) sampled on 7 April had generally higher methane concentrations and isotope signatures (72.3 nmol $kg^{-1}$ to 144.3 nmol $kg^{-1}$, -54.4‰ to -62.0‰) than ice core 2 (IC2) sampled on 15 April (53.3 nmol $kg^{-1}$ to 77.6 nmol $kg^{-1}$, -59.0‰ to -61.6‰). Microbial activity during storage of IC1 at 5°C for one week before analysis might have led to the differences in methane

concentrations and isotope ratios. Cell counts performed on IC2 showed an increase versus ice depth from 1.0 x $10^4$ cells $mL^{-1}$ in the top layers to 8.2 x $10^5$ cells $mL^{-1}$ in the bottom two cm of the ice core.

### 3.3 Oxidation rates and isotope fractionation during oxidation

The methane oxidation potential of microbial seawater communities at stations EL and IMB was determined from the methane mass balance in spiked incubation experiments (Table 3). Final dissolved methane concentrations ranged between 3.0 and 4000 nmol $L^{-1}$ representing approximately 0.2x to 200x the in situ concentration. Oxygen concentrations at the end of the long incubations ranged between 116% and 126% saturation, while oxygen concentration at the end of the short incubations was not determined.

Oxidation rates were published in Uhlig and Loose (2017) but are summarized here for comparison with microbial community structure. Short incubations (≤10 days) did not show significant oxidation, while long term incubations (41–46 days) did. Surprisingly, four out of five replicates of treatment 0.2x IMB showed a statistically significant increase in methane of about 0.62 ± 0.21 nmol $L^{-1}$ (N=5) within 10 days (Supplementary Figure 3). In long incubation samples with significant methane oxidation (10x and 200x spikes), the isotopic signature of the residual methane increased toward heavier (more positive) signatures with fractionation factors α of 1.0230 (10x EL), 1.0225 (10x IMB) and 1.0103 (200x IMB).

### 3.4 Bacterial community structure

The V4V5 region of the 16S rRNA was sequenced from a total of 10 seawater samples and 7 ice samples (Table 2). The seawater communities did not show gradients between sample dates or water depths. Proteobacteria were dominant with relative sequence abundances of 65.5% ± 2.5 % and 59.5% for IMB (N=9) and EL (N=1), respectively (Supplementary Figure 4). Within the phylum of Proteobaceteria, α- and γ-Proteobacteria made up the majority. The second most abundant phylum was Bacteriodetes with 19.6% ± 1.4% and 23%, for IMB and EL, respectively.

Similar to the seawater, sea ice (N=7) showed a dominance in Proteobacteria (58.9% ± 9.8%), but Bacteriodetes sequences (29.1% ± 11.7%) were slightly more abundant in the ice than in the water. γ-Proteobacteria dominated in all but one sample (IC2 30–46 cm). This one sample, which had clearly visible sediment included into the sea ice structure, was dominated by α-Proteobacteria.

In all incubated samples that were sequenced (N=10), species richness decreased (Figure 3) and the communities shifted toward higher fractions of γ-Proteobacteria over time. In short incubations (5–10 days; N=5) γ-Proteobacteria dominated with 61.8% ± 2.9% of sequences, while reaching 81.0% ± 11.1% in long incubated samples (41–46 days; N=4). In particular, one operational taxonomical unit (OTU), from the genus *Oleispira*, was very abundant in the long incubation time samples, with 50.1 to 76.3%, compared to abundances <0.04% in the in situ samples. The same OTU was only slightly more abundant in the short incubated treatments (0.5%–1.6%). In addition to the shift in community structure, total cell densities increased to 1.9 x 105 and 3.3 x 106 cells $mL^{-1}$ for short and long incubations, respectively, based on flow cytometric cell counts.

NMDS of the Bray-Curtis diversity revealed a high similarity across all of the in situ water samples that were analyzed for 16S diversity (Figure 4). Communities in the short incubation treatments (5–10 days; 0.2x, 2x, 200x short) were similar to the in situ samples, while the long incubations (41–46 days; 10x, 200x long) deviated further. Microbial communities in ice cores clearly separated from the water samples and were more distant to each other than the water samples.

### 3.5 Methanotrophs, methylotrophs and differentially abundant OTUs

Using their taxonomic annotation, we identified six groups of aerobic methanotrophs (MOB) (Figure 5). With a maximum of 1.76% ± 0.73% the relative abundance of MOB was low in all samples (Table 4). Four MOB grouped in the Methylococcales (γ-Proteobacteria), specifically Marine Methylotrophic Group 1 and 2 (MMG1, MMG2), unclassified Methlyococcales and the Milano-WF1B-03 family. The three remaining MOB OTUs belonged to the genera *Methylobacterium* and *Methyloceanibacter* (α-Proteobacteria) and *Candidatus "Methylacidiphilum"* (Verrucomicrobia). MOB OTUs were more abundant in natural seawater samples than in sea ice (maximal 0.11% in IC1 0–16 cm), but in contrast to the seawater, α-Proteobacteria MOB dominated in the sea ice.

Furthermore, four clades of non-methane utilizing methylotrophs (non-MOB methylotrophs) were identified, grouping into γ-Proteobacteria Marine Methylotrophic Group 3 (MMG3) and *Methylophaga*, and to the β-Proteobacteria Methylophilaceae (*Methylotenera*, OM43 clade). Non-MOB methylotroph OTUs were more abundant than MOB OTUs with exception of the 200x incubation treatments (Figure 5, Table 4). Ice samples showed the largest difference in abundance between non-MOB methylotrophs and MOB, with a ratio of 21:1 between the two OTUs. Ice samples also had the highest overall relative abundance of methylotrophs (MOB and non-MOB) of all in situ samples (max: 1.63%, IC1 0–16 cm). Only the 200x long incubation had a higher total number of methylotrophs (3.3%), while this sample was in addition dominated by MOB (2.49%). The second highest relative abundance of MOB was found for in situ IMB and EL with 0.24% ± 0.09% (N=10).

Taking into account the total cell number, a strong increase of MOB groups MMG1 (100 times) and Milano-WF1B-03 (10 times) was observed for the 10x and 200x long incubated samples compared to in situ conditions (Figure 5b).

Taxonomic groups that became differentially more abundant in the spiked samples than in natural communities were the y-Proteobacteria *Oleispira*, *Colwellia* and *Glaciecola* as well as Rhodobacteracea (α-Proteobacteria). Except for *Oleispira*, which became dominant, the other taxa had relative sequence read abundances from 1.1% to 12.6% after the oxidation experiments, compared to abundances <0.25% in in situ samples (Supplementary Figure 5).

### 3.6 Particulate methane monooxygenase (*pmoA*) sequences

A 225 base pair section of the particulate methane monooxgenase gene (*pmoA*) was sequenced in a total of 15 samples (Table 2). The absolute abundance of *pmoA* fragments ranged from 9331 (IMB in situ, 6.5 m depth) to 72781 (IMB 200x long) reads. In general, incubations with higher methane concentration had more *pmoA* reads than incubations with lower methane concentration and in situ. About three times more reads were filtered from the Elson Lagoon in situ sample (33844 reads, N=1) than the IMB in situ samples (11700 ± 1833, N=4).

Two of the 59 *pmoA* OTUs made up 96.8% of all sequences, while all other OTUs each represented ≤1% of the *pmoA* sequences. The most abundant OTU (71.0% of all sequences) clustered with two uncultured isolates from methane seeps (NCBI accession: HQ738559, EU444875) in the deep see-3/OPU3 subgroup of γ-Proteobacteria Type I MOB (Hansman et al., 2017; Knief, 2015; Lüke and Frenzel, 2011). The second most abundant (25.8%) OTU was related to *Methyloprofundus sedimentii*, another Type I MOB. Most of the low abundance OTUs also clustered within the Type I MOB, while only three OTUs (0.07% of all *pmoA* sequences) clustered with Type II α-Proteobacteria MOB *pmoA* sequences (*Methylocystis*, *Methylosinus*).

## 4 Discussion

### 4.1 Methane concentration and stable isotope ratios in seawater and ice

Seawater methane concentrations in April 2016 close to Utqiagvik Alaska were supersaturated 250% to 700% compared to levels at atmospheric equilibrium (3.6 nmol $L^{-1}$). The concentration at site EL (52.90 nmol $L^{-1}$, N=1) was in the range of a study by Lecher et al. (2016) in Elson Lagoon under ice free conditions (3.3–124.0 nmol $L^{-1}$). At site IMB concentrations were slightly lower (9.5 nmol $L^{-1}$ – 25.2 nmol $L^{-1}$: N=5) than previously reported from the same area for ice free (Lecher et al., 2016; mean: 40.6 nmol $L^{-1}$), and ice covered conditions (Zhou et al., 2014; March/April: 37.5 ± 6 nmol $L^{-1}$). Shallower depths exhibit lower methane concentrations (Figure 2), and the isotopic signature mirrors this pattern with more positive values toward the surface. This indicates that methane might be biologically oxidized on the way through the water column, after being released from the sediment.

The sea ice bulk methane concentrations observed in this study (53–144 nmol $kg^{-1}$) are significantly higher than in a study from the same area (Zhou et al., 2014), but fall within values reported for the Beaufort Sea (5 - 1260 nM, Lorenson and Kvenvolden, 1995). Methane carbon isotopic signatures (-54.4 to -63.8 ‰) are comparable to the higher end of previous studies for bulk sea ice (-52.1‰ to -83.4‰, Lorenson and Kvenvolden, 1995) and sea ice brine (-75‰, Damm et al., 2015). Although both ice cores were sampled within 300 m distance from each other at site IMB, they differ in concentration and isotope signature. The sediment at 30–46 cm depth in IC1, which was not observed in IC2, indicates that both ice cores have a different freezing history. Differences in methane concentration and isotope ratios could further have been caused by sample storage, which might have allowed for microbial activity, e.g. anaerobic methanogenesis, resulting in increasing methane concentrations. Ice algae derived organic carbon, which has a carbon isotopic signature of about -20‰ to -30‰ (e.g. Wang et al., 2014), could serve as substrate for methane production. Methane produced from this substrate would be enriched in $^{13}C$ (more positive) compared to the initial pool of methane (about -60‰ in IC2) and could explain the shift of the bulk methane isotopic signatures towards more positive values for IC1 (Figure 2, Figure 6). Sequences of bacterial taxa that might indicate anoxic conditions in the melted ice according to a study on an anoxic ice core (Eronen-Rasimus et al., 2017), were, however, not significantly more abundant in IC1 than in IC2 (Supplementary Table 2). An analysis of similarity (ANOSIM) between the two ice cores (not including the sediment influenced section), indicates that differences in the

community structure between the two ice cores are not significantly higher than within cores (ANOSIM: R=0.214, P=0.2). Thus, we thus cannot conclude if the differences in storage time or spatial variability led to the observed differences. Nevertheless, we assume that different microbial processes were taking place from the time of sea ice formation until measurement, which lead to the differences in methane concentration and stable isotope ratios.

Compared to the concentration in the underlying water column, methane concentrations in the sea ice sampled at station IMB were two to five times higher. In addition, the isotope signatures indicate less oxidized methane (-60.4 to -63.8 ‰) in most of the ice sections compared to the upper water column (-55%). In the Beaufort Sea, methane concentrations and isotopic signatures in sea ice were also found to be higher than values generally observed in the water column (Lorenson and Kvenvolden, 1995). In that region the high methane concentrations in fast ice – sea ice which is attached to the shore line - over the shallow shelf (<10 m water depth) were attributed to the inclusion of sedimentary sourced methane during the initial freezup (Lorenson et al., 2016). That this process also might have taken place in the fast ice sampled in this study, is supported by the fact that methane concentrations in IC2 are close to water column concentrations reported in previous studies for the same region (Lecher et al., 2016; Zhou et al., 2014). The lower sea water methane concentrations in our study, together with the more positive (heavier) isotopic signature compared to the ice, might indicate that the microbial community in the water column is oxidizing more methane during the ice covered period than in the freezup period. Higher oxidation rates during ice covered periods compared to ice free conditions were previously reported for the Beaufort Sea (Lorenson and Kvenvolden, 1995).

### 4.2 Methane cycling at different methane concentrations

Oxidation rates of the long incubation treatments at 10x and 200x methane concentration fall into the middle of rates published for Arctic and subarctic environments (Damm et al., 2015; Gentz et al., 2014; Lorenson et al., 2016; Mau et al., 2013, 2017; Steinle et al., 2015) or marine sites with high oxidation rates at oil spills or gas flares (Redmond et al., 2010; Valentine et al., 2010). The fractionation factors ($\alpha_{ox}$) that we observed with these oxidation rates were higher than reported from cold marine environments with a range of $\alpha_{ox}$ from 1.002 to 1.017 (Cowen et al., 2002; Damm et al., 2008; Grant and Whiticar, 2002; Heeschen et al., 2004; Keir et al., 2009; Tsunogai et al., 2000). Some of these fractionation factors, which were calculated from in situ data, might however be underestimated due to mixing effects in the water column (Grant and Whiticar, 2002). The fractionation factors observed in our study seem to be inversely dependent on the methane spike concentration, with a higher fractionation in the 50x (1.023, N=6) treatments than in the 200x (1.010, N=2) treatments. The relative and absolute abundances of MOB as well as the dominant MOB types differed between both treatments, possibly providing explanations to the differences in fractionation rates.

The short incubation 2x and 200x treatments did not show oxidation of methane. A longer incubation time would have been required for the 2x treatments to meet the sensitivity threshold for the applied method given the observed low oxidation rate constants in other samples (Uhlig and Loose, 2017). The 200x treatments were likely just about to leave the lag phase when the experiments were stopped after 7 days. A lag phase of 6 days was observed for the long incubation 200x samples, in

which the microbial community possibly to shifted towards an abundance of MOB that was large enough to cause detectable methane oxidation.

The increase in methane concentration in treatment IMB 0.2x (10 days incubation) is surprising since experiments were performed under aerobic conditions. We were, however, able to amplify the methyl coenzyme-M reductase (*mcrA*), a marker for anaerobic methane production, in all four IMB samples analyzed for it, including this incubation (1–480 sequences detected, data not shown). Since the seawater was not pre-filtered through a larger pore size filter, which would exclude larger particles but allow bacterial cells to pass, production of methane in microanoxic zones (de Angelis and Lee, 1994; Oremland, 1979) should be considered.

Furthermore, several studies suggested pathways for methane production in oxygenated marine systems, which use methylated substrates like dimethylsulfoniopropionate (DMSP), dimethylsulfide (DMS), methylphosphonate or other phosphonates in marine dissolved organic matter (Damm et al., 2010; Florez-Leiva et al., 2010; Karl et al., 2008; Repeta et al., 2016). The rich microalgal and bacterial community found at the underside of sea ice could be a source for DMSP and DMS (Kirst et al., 1991). Dissolved organic phosphate, which encompasses phosphonates, could originate from river runoff or sediment resuspension (Piper et al., 2016). In addition to biological processes, we cannot entirely rule out an abiotic effect leading to the increased methane concentrations, since our experimental setup did not include a killed control at the same methane concentration. The production rate of 0.06 nmol $L^{-1}$ $day^{-1}$ observed in our study is low compared to previously published methane production rates under aerobic conditions, which range between 5 and 4000 nmol $L^{-1}$ $day^{-1}$. The high rates in these studies were, however, obtained with the addition of high amounts of potential substrates DMSP and methylphosphonate (Damm et al., 2010; Karl et al., 2008), while in our study none of the possible substrates were added.

The 0.2x incubations, without addition of methane, had a dissolved methane concentration five times lower than the in situ methane concentration, as most methane would have degassed into the headspace. We hypothesize that in all other treatments the higher methane concentrations lead to oxidation rates which masked the methane production signal.

### 4.3 Abundances of MOB and non-MOB methylotrophs control the methane oxidation potential

We found a strong linear correlation between the bulk oxidation rate constant ($k_{ox}$) and the relative abundance of MOB sequences (Spearman rank order coefficient $\rho_s = 0.79$, p=0.006) (Figure 7, Table 5). This strong correlation is confirmed when correlating against the total abundance or DESeq2 normalized abundance of 16S MOB sequences (Table 5). The correlation to $k_{ox}$ was even stronger for the absolute abundance of *pmoA* sequences ($\rho_s = 0.86$, p=0.006) retrieved from the respective datasets. This presentation of a direct and statistically significant linear relationship is a first to our knowledge. It agrees with other qualitative reports of positive correlations between oxidation rates and abundance of *pmoA* or MOB 16S rRNA, determined using a variety of methods - quantitative PCR, FISH, or sequencing - for marine water column and lake sediments (Crespo-Medina et al., 2014; Deutzmann et al., 2011; e.g. Rahalkar et al., 2009; Steinle et al., 2015).

Cell specific oxidation rates in our study (3.2–7.5 fmol cell$^{-1}$ h$^{-1}$) were relatively constant between treatments. They are two orders of magnitude higher than reported for the subarctic marine environment (Steinle et al., 2016). Since the cell specific rates only span a narrow range, the ultimate control on the methane oxidation potential is the number of MOB.

Despite the long incubation time in our experiments and the fact that methane was the only added source of carbon, the relative abundance of MOB determined from 16S reads was low (<2.5%, Table 4). Other studies at natural or man-made gas or oil spills, with comparably high dissolved methane concentrations like in our 10x and 200x treatments, reported maximal values of 8 to 34% of MOB (Crespo-Medina et al., 2014; Kessler et al., 2011; Steinle et al., 2015, 2016). Surprisingly, relative sequence abundances of MOB in the natural seawater communities were higher than in the incubations except for the 200x treatment (Table 4). Inferred absolute MOB numbers were higher in 10x and 200x incubations than in in situ, while the low spiked samples were lower (Figure 5b), indicating that the provided methane concentration at 0.2x and 2x was too low to stimulate MOB growth.

It is puzzling why the fraction of methane oxidizers in the bacterial community did not increase above the observed low percentages although the cell specific oxidation rates were high and sufficient methane was available, particularly in the 10x and 200x treatments. Oxygen and methane can be ruled out as the limiting factor since both were abundant. Further, we consider copper as unlikely to be limiting, since *pmoA* is only expressed in the presence of copper, yet correlates with the $k_{ox}$. Additionally, we would expect an impact on the cell specific oxidation rate if and when copper restricted oxidation. Potentially the low relative abundance of MOB sequences is due to competition with other bacterial taxa for other macro- or micronutrients. In the absence of other added C substrates these other taxa could have been utilizing the initial pool of dissolved organic carbon (DOC). DOC concentration is about 68 µM carbon in the Southern Chukchi Sea (Tanaka et al., 2016), which is in the same range as the amount of consumed methane carbon in the 200x treatments and two orders of magnitude higher than the consumed carbon in the 10x treatments.

As a result of the low MOB abundances the potential of the microbial community to mitigate release of dissolved methane to the atmosphere by oxidation is small. For example, for methane concentrations in the Laptev Sea area, the rates observed in this study would result in 0.2% consumption during the ice covered period. This supports the results from a previous study for the Beaufort Sea where an amount of 1–2% of dissolved methane was calculated to be oxidized (Lorenson and Kvenvolden, 1997).

### 4.4 Structure of the methane degrading microbial community

This first 16S MiSeq sequencing based study on methane oxidizing sea water communities in the Arctic provides a broader view on the community structure than approaches with FISH and DGGE. The dominance of γ-Proteobacteria MOB in our natural and incubated seawater samples is in agreement with previous records on MOB diversity for polar and subpolar waters (Mau et al., 2013; Steinle et al., 2015; Verdugo et al., 2016). In addition, non-methane-utilizing methylotrophs were present in all of our samples. The relative read abundance of non-MOB methylotrophs were, similar to MOB, tightly correlated to $k_{ox}$, and the same correlation holds for the relative abundance of total methylotrophs (MOB plus non-MOB).

The correlation is, however, weak for the OTUs that were differentially more abundant in the incubated samples (Table 5). This points toward a possible link between the MOB and non-MOB in this methane oxidizing microbial community and that non-MOB methylotrophs might play a role for community methane oxidation, whereas the OTUs that were differentially more abundant, are not directly linked to methane oxidation.

Methylophilacaea, the most abundant non-MOB methylotroph in our experiments, have been found to be abundant in sediment methane oxidizing communities in lakes and marine systems (Beck et al., 2013; Redmond et al., 2010). A possible cooperative behavior between methanotrophs (Methylococcacaea) and non-MOB methylotrophs (Methylophilaceae) was suggested (Beck et al., 2013), in which the latter cross-feeds on intermediate metabolic products of the MOB, i.e. methanol, and can even positively alter the metabolism of the MOB towards methane assimilation (Krause et al., 2017).

To test if the non-methane MOB could be supported by the intermediate substrates produced by MOB, we calculated a budget between the methane carbon assimilated by the growing microbial population ($C_{CH_4,assim}$), and the cell-carbon gained during growth ($C_{cell-growth}$) (Figure 8). We assumed a cellular carbon content of 150 fg for exponentially growing bacterial cells (Vrede et al., 2002) and that about 1/3 of consumed $CH_4$-carbon is assimilated, while the remaining 2/3 are respired to $CO_2$ (Bastviken et al., 2003; Roslev et al., 1997). $C_{CH_4,assim}$ exceeds MOB-$C_{cell-growth}$ by y factor of 9 to 17, indicating that some of the $C_{CH_4,assim}$ was available for secondary consumption by non-MOB. The entire methylotrophic community (MOB + non-MOB-methylotroph) growth can also be explained solely by $C_{CH_4,assim}$, supporting the possible link of non-MOB methylotrophs to methane consumption. In contrast, only about 0.1% of the total community growth could be supported by $C_{CH_4,assim}$ in the 10x treatment and 15% in the 200x treatment. The remaining cell growth must have been supported by other carbon sources, like initially available DOC.

### 4.5 MOB and methylotrophs in sea ice

The two sea ice cores analyzed in this study give a first insight on the possible role of methane oxidizers in sea ice. In contrast to seawater samples, MOB found in sea ice samples were mostly α-Proteobacteria. The relative sequence read abundance of MOB in the ice was very low (maximal 0.1%) pointing to an overall low contribution of methane oxidation inside sea ice. The highest abundances of MOB were found in the top most ice sections of both ice core (Figure 5b) coinciding with the highest methane concentration in case of IC2 (Figure 2e). Abundances in the inner and bottom sections were one to two orders of magnitude lower or in case of the biologically rich bottom section of IC2, no typical MOB were identified at all.

The biologically rich bottom section of IC2 and the top section of IC1 had the highest abundance of β-Proteobacteria Methylophilaceae, a non-MOB methylotroph. Recently identified as DMS degraders (Eyice et al., 2015), Methylophilaceae might use DMS, a methylated compound abundant in sea ice, as substrate (Kirst et al., 1991).

## 5 Conclusions

We studied the structure and methane oxidation potential of microbial communities from Arctic seawater and sea ice. The natural seawater community had relative sequence abundances of MOB of 0.24% ± 0.09% and was dominated by γ-Proteobacteria MOB, while α-Proteobacteria MOB dominated in sea ice with maximal fractions of ≤0.1% in the surface of the sea ice. In seawater incubations under different methane concentrations the overall relative abundance of methane oxidizers (MOB) was low with a maximum of 2.5% and the dominant MOB types were γ-Proteobacteria. A tight correlation between the rate constant of methane oxidation and relative abundance of MOB and as well non-MOB methylotrophs suggests that (1) the abundance of MOB is a control on the magnitude of methane oxidation and (2) non-MOB methylotrophs might play a role in methane oxidation, possibly by interacting with the MOB. The low abundance of MOB, despite ample methane availability, and role of methylotrophs in methane oxidation, are both open questions.

Higher methane concentrations in the sea ice compared to the underlying water and an offset in stable isotope ratios, suggest that either fractionation and solute concentration occurred during freeze up, or different microbial processes took place within the ice and water. Possible processes could be microbial production of methane, even within the ice (Damm et al., 2015), or microbial oxidation in the water column. To address these hypotheses, future studies should directly compare both sea ice and water, particularly during ice freeze up, and involve investigation of the microbial processes.

## Acknowledgements

This work was supported the American Chemical Society, Petroleum Research Fund (PRF# 54473-DNI2). Part of this research is based upon work conducted using the NSF EPSCoR Marine Science Research Facility and Rhode Island NSF EPSCoR Genomics and Sequencing Center, which are supported in part by the National Science Foundation under EPSCoR Grants Nos. 0554548 and EPS-1004057. We thank Clarisse Sullivan for support with preparations for fieldwork and Rodrigue Spinette for help with flow cytometry and qPCR as well as the nutrient measurements. We would like to thank David C. Smith and Lucy Maranda for borrowing equipment and discussing concepts and experimental procedures.

## References

Andrews, S.: FastQC: a quality control tool for high throughput sequence data. Available online at: http://www.bioinformatics.babraham.ac.uk/projects/fastqc (Accessed 29 September 2017), 2010.

de Angelis, M. A. and Lee, C.: Methane production during zooplankton grazing on marine phytoplankton, Limnol. Oceanogr., 39(6), 1298–1308, doi:10.4319/lo.1994.39.6.1298, 1994.

Barnes, R. O. and Goldberg, E. D.: Methane production and consumption in anoxic marine sediments, Geology, 4(5), 297, doi:10.1130/0091-7613(1976)4<297:MPACIA>2.0.CO;2, 1976.

Bastviken, D., Ejlertsson, J., Sundh, I. and Tranvik, L.: Methane as a Source of Carbon and Energy for Lake Pelagic Food Webs, Ecology, 84(4), 969–981, 2003.

Beck, D. A. C., Kalyuzhnaya, M. G., Malfatti, S., Tringe, S., Glavina del Rio, T., Ivanova, N., Lidstrom, M. and Chistoserdova, L.: A metagenomic insight into freshwater methane-utilizing communities and evidence for cooperation between the *Methylococcaceae* and the *Methylophilaceae*, PeerJ, 1, e23, doi:10.7717/peerj.23, 2013.

Boetius, A. and Wenzhöfer, F.: Seafloor oxygen consumption fuelled by methane from cold seeps, Nat. Geosci., 6(9), 725–734, doi:10.1038/ngeo1926, 2013.

Coleman, D. D., Risatti, J. B. and Schoell, M.: Fractionation of carbon and hydrogen isotopes by methane-oxidizing bacteria, Geochim. Cosmochim. Acta, 45(7), 1033–1037, doi:10.1016/0016-7037(81)90129-0, 1981.

Cowen, J. P., Wen, X. and Popp, B. N.: Methane in aging hydrothermal plumes, Geochim. Cosmochim. Acta, 66(20), 3563–3571, doi:10.1016/S0016-7037(02)00975-4, 2002.

Cox, G. F. N. and Weeks, W. F.: Equations for determining the gas and brine volumes in sea-ice samples, J. Glaciol., 29(102), 306–316, 1983.

Crespo-Medina, M., Meile, C. D., Hunter, K. S., Diercks, A.-R., Asper, V. L., Orphan, V. J., Tavormina, P. L., Nigro, L. M., Battles, J. J., Chanton, J. P., Shiller, A. M., Joung, D.-J., Amon, R. M. W., Bracco, A., Montoya, J. P., Villareal, T. A., Wood, A. M. and Joye, S. B.: The rise and fall of methanotrophy following a deepwater oil-well blowout, Nat. Geosci., 7(6), 423–427, doi:10.1038/ngeo2156, 2014.

Damm, E., Mackensen, A., Budéus, G., Faber, E. and Hanfland, C.: Pathways of methane in seawater: Plume spreading in an Arctic shelf environment (SW-Spitsbergen), Cont. Shelf Res., 25(12–13), 1453–1472, doi:10.1016/j.csr.2005.03.003, 2005.

Damm, E., Kiene, R. P., Schwarz, J., Falck, E. and Dieckmann, G.: Methane cycling in Arctic shelf water and its relationship with phytoplankton biomass and DMSP, Mar. Chem., 109(1–2), 45–59, doi:10.1016/j.marchem.2007.12.003, 2008.

Damm, E., Helmke, E., Thoms, S., Schauer, U., Nöthig, E., Bakker, K. and Kiene, R. P.: Methane production in aerobic oligotrophic surface water in the central Arctic Ocean, Biogeosciences, 7(3), 1099–1108, doi:10.5194/bg-7-1099-2010, 2010.

Damm, E., Rudels, B., Schauer, U., Mau, S. and Dieckmann, G.: Methane exess in Arctic surface water- triggered by sea ice formation and melting, Sci. Rep., 2015.

Deutzmann, J. S., Worner, S. and Schink, B.: Activity and Diversity of Methanotrophic Bacteria at Methane Seeps in Eastern Lake Constance Sediments, Appl. Environ. Microbiol., 77(8), 2573–2581, doi:10.1128/AEM.02776-10, 2011.

Dunfield, P. F., Yuryev, A., Senin, P., Smirnova, A. V., Stott, M. B., Hou, S., Ly, B., Saw, J. H., Zhou, Z., Ren, Y., Wang, J., Mountain, B. W., Crowe, M. A., Weatherby, T. M., Bodelier, P. L. E., Liesack, W., Feng, L., Wang, L. and Alam, M.: Methane oxidation by an extremely acidophilic bacterium of the phylum Verrucomicrobia, Nature, 450(7171), 879–882, doi:10.1038/nature06411, 2007.

Edgar, R. C., Haas, B. J., Clemente, J. C., Quince, C. and Knight, R.: UCHIME improves sensitivity and speed of chimera detection, Bioinformatics, 27(16), 2194–2200, doi:10.1093/bioinformatics/btr381, 2011.

Eronen-Rasimus, E., Luhtanen, A.-M., Rintala, J.-M., Delille, B., Dieckmann, G., Karkman, A. and Tison, J.-L.: An active bacterial community linked to high chl-a concentrations in Antarctic winter-pack ice and evidence for the development of an anaerobic sea-ice bacterial community, ISME J., doi:10.1038/ismej.2017.96, 2017.

Eyice, Ö., Namura, M., Chen, Y., Mead, A., Samavedam, S. and Schäfer, H.: SIP metagenomics identifies uncultivated Methylophilaceae as dimethylsulphide degrading bacteria in soil and lake sediment, ISME J., 9(11), 2336–2348, doi:10.1038/ismej.2015.37, 2015.

Fish, J. A., Chai, B., Wang, Q., Sun, Y., Brown, C. T., Tiedje, J. M. and Cole, J. R.: FunGene: the functional gene pipeline and repository, Front. Microbiol., 4, doi:10.3389/fmicb.2013.00291, 2013.

Florez-Leiva, L., Tarifeño, E., Cornejo, M., Kiene, R. and Farías, L.: High production of nitrous oxide ($N_2O$), methane ($CH_4$) and dimethylsulphoniopropionate (DMSP) in a massive marine phytoplankton culture, Biogeosciences Discuss., 7(5), 6705–6723, doi:10.5194/bgd-7-6705-2010, 2010.

Formolo, M.: The microbial production of methane and other volatile hydrocarbons, in Handbook of Hydrocarbon and Lipid Microbiology, edited by K. N. Timmis, pp. 113–126, Springer Berlin Heidelberg, Berlin, Heidelberg. [online] Available from: http://link.springer.com/10.1007/978-3-540-77587-4_6 (Accessed 5 January 2017), 2010.

Gentz, T., Damm, E., Schneider von Deimling, J., Mau, S., McGinnis, D. F. and Schlüter, M.: A water column study of methane around gas flares located at the West Spitsbergen continental margin, Cont. Shelf Res., 72, 107–118, doi:10.1016/j.csr.2013.07.013, 2014.

Golden, K. M., Ackley, S. F. and Lytle, V. I.: The Percolation Phase Transition in Sea Ice, Science, 282(5397), 2238–2241, doi:10.1126/science.282.5397.2238, 1998.

Grant, N. J. and Whiticar, M. J.: Stable carbon isotopic evidence for methane oxidation in plumes above Hydrate Ridge, Cascadia Oregon Margin., Glob. Biogeochem. Cycles, 16(4), 71-1-71–13, doi:10.1029/2001GB001851, 2002.

Hansman, R. L., Thurber, A. R., Levin, L. A. and Aluwihare, L. I.: Methane fates in the benthos and water column at cold seep sites along the continental margin of Central and North America, Deep Sea Res. Part Oceanogr. Res. Pap., 120, 122–131, doi:10.1016/j.dsr.2016.12.016, 2017.

Hanson, R. S. and Hanson, T. E.: Methanotrophic bacteria, Microbiol. Rev., 60(2), 439–471, 1996.

Heeschen, K. U., Keir, R. S., Rehder, G., Klatt, O. and Suess, E.: Methane dynamics in the Weddell Sea determined via stable isotope ratios and CFC-11, Glob. Biogeochem. Cycles, 18(2), n/a-n/a, doi:10.1029/2003GB002151, 2004.

Holmes, A. J., Roslev, P., McDonald, I. R., Iversen, N., Henriksen, K. and Murrell, J. C.: Characterization of Methanotrophic Bacterial Populations in Soils Showing Atmospheric Methane Uptake, Appl. Environ. Microbiol., 65(8), 3312–3318, 1999.

Hutchens, E., Radajewski, S., Dumont, M. G., McDonald, I. R. and Murrell, J. C.: Analysis of methanotrophic bacteria in Movile Cave by stable isotope probing: Methanotrophs in Movile Cave, Environ. Microbiol., 6(2), 111–120, doi:10.1046/j.1462-2920.2003.00543.x, 2003.

IPCC: Climate Change 2014: Mitigation of Climate Change. Contribution of Working Group III to the Fifth Assessment Report of the Intergovernmental Panel on Climate Change. Edenhofer, O., Pichs-Madruga, R., Sokona, Y., Farahani, E., Kadner, S., Seyboth, K., Adler, A., Baum, I., Brunner, S., Eickemeier, P., Kriemann, B., Savolainen, J., Schlömer, S., von Stechow, C., Zwickel, T., Minx J.C. (Eds). Cambridge University Press, Cambridge, United Kingdom and New York, NY, USA., 2014.

Jensen, S., Neufeld, J. D., Birkeland, N.-K., Hovland, M. and Murrell, J. C.: Methane assimilation and trophic interactions with marine Methylomicrobium in deep-water coral reef sediment off the coast of Norway: Deep-water coral reef methanotrophy, FEMS Microbiol. Ecol., 66(2), 320–330, doi:10.1111/j.1574-6941.2008.00575.x, 2008.

Karl, D. M., Beversdorf, L., Björkman, K. M., Church, M. J., Martinez, A. and Delong, E. F.: Aerobic production of methane in the sea, Nat. Geosci., 1(7), 473–478, 2008.

Katoh, K. and Standley, D. M.: MAFFT Multiple Sequence Alignment Software Version 7: Improvements in Performance and Usability, Mol. Biol. Evol., 30(4), 772–780, doi:10.1093/molbev/mst010, 2013.

Keir, R. S., Schmale, O., Seifert, R. and Sültenfuß, J.: Isotope fractionation and mixing in methane plumes from the Logatchev hydrothermal field, Geochem. Geophys. Geosystems, 10(5), n/a-n/a, doi:10.1029/2009GC002403, 2009.

Kessler, J. D., Valentine, D. L., Redmond, M. C., Du, M., Chan, E. W., Mendes, S. D., Quiroz, E. W., Villanueva, C. J., Shusta, S. S., Werra, L. M., Yvon-Lewis, S. A. and Weber, T. C.: A Persistent Oxygen Anomaly Reveals the Fate of Spilled Methane in the Deep Gulf of Mexico, Science, 331(6015), 312–315, doi:10.1126/science.1199697, 2011.

Kirst, G. O., Thiel, C., Wolff, H., Nothnagel, J., Wanzek, M. and Ulmke, R.: Dimethylsulfoniopropionate (DMSP) in ice-algae and its possible biological role, Mar. Chem., 35(1–4), 381–388, doi:10.1016/S0304-4203(09)90030-5, 1991.

Knief, C.: Diversity and Habitat Preferences of Cultivated and Uncultivated Aerobic Methanotrophic Bacteria Evaluated Based on pmoA as Molecular Marker, Front. Microbiol., 6, doi:10.3389/fmicb.2015.01346, 2015.

Knittel, K. and Boetius, A.: Anaerobic oxidation of methane: Progress with an unknown process, Annu. Rev. Microbiol., 63(1), 311–334, doi:10.1146/annurev.micro.61.080706.093130, 2009.

Krause, S. M. B., Johnson, T., Samadhi Karunaratne, Y., Fu, Y., Beck, D. A. C., Chistoserdova, L. and Lidstrom, M. E.: Lanthanide-dependent cross-feeding of methane-derived carbon is linked by microbial community interactions, Proc. Natl. Acad. Sci., 114(2), 358–363, doi:10.1073/pnas.1619871114, 2017.

Kvenvolden, K. A. and Rogers, B. W.: Gaia's breath—global methane exhalations, Mar. Pet. Geol., 22(4), 579–590, doi:10.1016/j.marpetgeo.2004.08.004, 2005.

Larkin, M. A., Blackshields, G., Brown, N. P., Chenna, R., McGettigan, P. A., McWilliam, H., Valentin, F., Wallace, I. M., Wilm, A., Lopez, R., Thompson, J. D., Gibson, T. J. and Higgins, D. G.: Clustal W and Clustal X version 2.0, Bioinformatics, 23(21), 2947–2948, doi:10.1093/bioinformatics/btm404, 2007.

Lecher, A. L., Kessler, J., Sparrow, K., Garcia-Tigreros Kodovska, F., Dimova, N., Murray, J., Tulaczyk, S. and Paytan, A.: Methane transport through submarine groundwater discharge to the North Pacific and Arctic Ocean at two Alaskan sites, Limnol. Oceanogr., 61(S1), S344–S355, doi:10.1002/lno.10118, 2016.

Leifer, I. and Patro, R. K.: The bubble mechanism for methane transport from the shallow sea bed to the surface: A review and sensitivity study, Cont. Shelf Res., 22(16), 2409–2428, doi:http://dx.doi.org/10.1016/S0278-4343(02)00065-1, 2002.

Loose, B., Schlosser, P., Perovich, D., Ringelberg, D., Ho, D. T., Takahashi, T., Richter-Menge, J., Reynolds, C. M., Mcgillis, W. R. and Tison, J.-L.: Gas diffusion through columnar laboratory sea ice: implications for mixed-layer ventilation of $CO_2$ in the seasonal ice zone., Tellus B, 63(1), 23–39, doi:10.1111/j.1600-0889.2010.00506.x, 2011.

Lorenson, T. D. and Kvenvolden, K. A.: Methane in coastal seawater, sea ice and bottom sediments, Beaufort Sea, Alaska: U.S. Geological Survey Open-File Report 95-70, US Geological Survey, Menlo Park, CA, 1995.

Lorenson, T. D. and Kvenvolden, K. A.: Methane in coastal sea water, sea ice, and bottom sediments, Beaufort Sea, Alaska-results from 1995. U.S. Geological Survey Open-File Report 97-54, 77 p., 1997.

Lorenson, T. D., Greinert, J. and Coffin, R. B.: Dissolved methane in the Beaufort Sea and the Arctic Ocean, 1992-2009; sources and atmospheric flux: Dissolved methane in the Beaufort Sea and the Arctic Ocean, Limnol. Oceanogr., 61(S1), S300–S323, doi:10.1002/lno.10457, 2016.

Love, M. I., Huber, W. and Anders, S.: Moderated estimation of fold change and dispersion for RNA-seq data with DESeq2, Genome Biol., 15(12), doi:10.1186/s13059-014-0550-8, 2014.

Lüke, C. and Frenzel, P.: Potential of pmoA Amplicon Pyrosequencing for Methanotroph Diversity Studies, Appl. Environ. Microbiol., 77(17), 6305–6309, doi:10.1128/AEM.05355-11, 2011.

Lyew, D. and Guiot, S.: Effects of aeration and organic loading rates on degradation of trichloroethylene in a methanogenic-methanotrophic coupled reactor, Appl. Microbiol. Biotechnol., 61(3), 206–213, doi:10.1007/s00253-003-1224-8, 2003.

Magen, C., Lapham, L. L., Pohlman, J. W., Marshall, K., Bosman, S., Casso, M. and Chanton, J. P.: A simple headspace equilibration method for measuring dissolved methane, Limnol. Oceanogr. Methods, 12(9), 637–650, doi:10.4319/lom.2014.12.637, 2014.

Mau, S., Blees, J., Helmke, E., Niemann, H. and Damm, E.: Vertical distribution of methane oxidation and methanotrophic response to elevated methane concentrations in stratified waters of the Arctic fjord Storfjorden (Svalbard, Norway), Biogeosciences, 10(10), 6267–6278, doi:10.5194/bg-10-6267-2013, 2013.

Mau, S., Römer, M., Torres, M. E., Bussmann, I., Pape, T., Damm, E., Geprägs, P., Wintersteller, P., Hsu, C.-W., Loher, M. and Bohrmann, G.: Widespread methane seepage along the continental margin off Svalbard - from Bjørnøya to Kongsfjorden, Sci. Rep., 7, 42997, doi:10.1038/srep42997, 2017.

McDonald, I. R., Bodrossy, L., Chen, Y. and Murrell, J. C.: Molecular Ecology Techniques for the Study of Aerobic Methanotrophs, Appl. Environ. Microbiol., 74(5), 1305–1315, doi:10.1128/AEM.02233-07, 2008.

McKinney, C. R., McCrea, J. M., Epstein, S., Allen, H. A. and Urey, H. C.: Improvements in mass spectrometers for the measurement of small differences in isotope abundance ratios, Rev. Sci. Instrum., 21(8), 724, doi:10.1063/1.1745698, 1950.

McMurdie, P. J. and Holmes, S.: phyloseq: An R Package for Reproducible Interactive Analysis and Graphics of Microbiome Census Data, PLoS ONE, 8(4), e61217, doi:10.1371/journal.pone.0061217, 2013.

Murrell, J. C.: The aerobic methane oxidizing bacteria (Methanotrophs), in Handbook of Hydrocarbon and Lipid Microbiology, edited by K. N. Timmis, pp. 1953–1966, Springer Berlin Heidelberg, Berlin, Heidelberg. [online] Available from: http://link.springer.com/10.1007/978-3-540-77587-4_143 (Accessed 5 January 2017), 2010.

Nelson, M. C., Morrison, H. G., Benjamino, J., Grim, S. L. and Graf, J.: Analysis, Optimization and Verification of Illumina-Generated 16S rRNA Gene Amplicon Surveys, PLoS ONE, 9(4), e94249, doi:10.1371/journal.pone.0094249, 2014.

Oksanen, J., Blanchet, F. G., Friendly, M., Kindt, R., Legendre, P., McGlinn, D., Minchin, P. R., O'Hara, R. B., Simpson, G. L., Solymos, P., Stevens, M. H. H., Szoecs, E. and Wagner, H.: vegan: Community Ecology Package. [online] Available from: https://CRAN.R-project.org/package=vegan, 2017.

Oremland, R. S.: Methanogenic activity in plankton samples and fish intestines: A mechanism for in situ methanogenesis in oceanic surface waters, Limnol. Oceanogr., 24(6), 1136–1141, doi:10.4319/lo.1979.24.6.1136, 1979.

Overduin, P. P., Westermann, S., Yoshikawa, K., Haberlau, T., Romanovsky, V. and Wetterich, S.: Geoelectric observations of the degradation of nearshore submarine permafrost at Barrow (Alaskan Beaufort Sea), J. Geophys. Res. Earth Surf., 117(F2), n/a-n/a, doi:10.1029/2011JF002088, 2012.

Piper, M. M., Benitez-Nelson, C. R., Frey, K. E., Mills, M. M. and Pal, S.: Dissolved and particulate phosphorus distributions and elemental stoichiometry throughout the Chukchi Sea, Deep Sea Res. Part II Top. Stud. Oceanogr., 130, 76–87, doi:10.1016/j.dsr2.2016.05.009, 2016.

Pol, A., Heijmans, K., Harhangi, H. R., Tedesco, D., Jetten, M. S. M. and Op den Camp, H. J. M.: Methanotrophy below pH 1 by a new Verrucomicrobia species, Nature, 450(7171), 874–878, doi:10.1038/nature06222, 2007.

Preuss, I., Knoblauch, C., Gebert, J. and Pfeiffer, E.-M.: Improved quantification of microbial $CH_4$ oxidation efficiency in arctic wetland soils using carbon isotope fractionation, Biogeosciences, 10(4), 2539–2552, doi:10.5194/bg-10-2539-2013, 2013.

Quast, C., Pruesse, E., Yilmaz, P., Gerken, J., Schweer, T., Yarza, P., Peplies, J. and Glockner, F. O.: The SILVA ribosomal RNA gene database project: improved data processing and web-based tools, Nucleic Acids Res., 41(D1), D590–D596, doi:10.1093/nar/gks1219, 2013.

R CoreTeam: R: A language and Environment for Statistical Computing. Available at: http://www.r-project.org/, 2015.

Rahalkar, M., Deutzmann, J., Schink, B. and Bussmann, I.: Abundance and Activity of Methanotrophic Bacteria in Littoral and Profundal Sediments of Lake Constance (Germany), Appl. Environ. Microbiol., 75(1), 119–126, doi:10.1128/AEM.01350-08, 2009.

Redmond, M. C., Valentine, D. L. and Sessions, A. L.: Identification of Novel Methane-, Ethane-, and Propane-Oxidizing Bacteria at Marine Hydrocarbon Seeps by Stable Isotope Probing, Appl. Environ. Microbiol., 76(19), 6412–6422, doi:10.1128/AEM.00271-10, 2010.

Reeburgh, W. S.: Methane consumption in Cariaco Trench waters and sediments, Earth Planet. Sci. Lett., 28(3), 337–344, doi:10.1016/0012-821X(76)90195-3, 1976.

Reeburgh, W. S.: Oceanic methane biogeochemistry, Chem. Rev., 107, 486–513, 2007.

Reeburgh, W. S., Ward, B. B., Whalen, S. C., Sandbeck, K. A., Kilpatrickt, K. A. and Kerkhof, L. J.: Black Sea methane geochemistry, Deep Sea Res. Part Oceanogr. Res. Pap., 38, S1189–S1210, doi:10.1016/S0198-0149(10)80030-5, 1991.

Repeta, D. J., Ferron, S., Sosa, O. A., Johnson, C. G., Repeta, L. D., Acker, M., DeLong, E. F. and Karl, D. M.: Marine methane paradox explained by bacterial degradation of dissolved organic matter, Nat. Geosci, 9(12), 884–887, 2016.

Rice, P., Longden, I. and Bleasby, A.: EMBOSS: The European Molecular Biology Open Software Suite, Trends Genet., 16(6), 276–277, doi:10.1016/S0168-9525(00)02024-2, 2000.

Roslev, P., Iversen, N. and Henriksen, K.: Oxidation and assimilation of atmospheric methane by soil methane oxidizers., Appl. Environ. Microbiol., 63(3), 874–880, 1997.

Saidi-Mehrabad, A., He, Z., Tamas, I., Sharp, C. E., Brady, A. L., Rochman, F. F., Bodrossy, L., Abell, G. C., Penner, T., Dong, X., Sensen, C. W. and Dunfield, P. F.: Methanotrophic bacteria in oilsands tailings ponds of northern Alberta, ISME J., 7(5), 908–921, doi:10.1038/ismej.2012.163, 2013.

Sansone, F. J., Popp, B. N., Gasc, A., Graham, A. W. and Rust, T. M.: Highly elevated methane in the eastern tropical North Pacific and associated isotopically enriched fluxes to the atmosphere, Geophys. Res. Lett., 28(24), 4567–4570, doi:10.1029/2001GL013460, 2001.

Saunois, M., Bousquet, P., Poulter, B., Peregon, A., Ciais, P., Canadell, J. G., Dlugokencky, E. J., Etiope, G., Bastviken, D., Houweling, S., Janssens-Maenhout, G., Tubiello, F. N., Castaldi, S., Jackson, R. B., Alexe, M., Arora, V. K., Beerling, D. J., Bergamaschi, P., Blake, D. R., Brailsford, G., Brovkin, V., Bruhwiler, L., Crevoisier, C., Crill, P., Covey, K., Curry, C., Frankenberg, C., Gedney, N., Höglund-Isaksson, L., Ishizawa, M., Ito, A., Joos, F., Kim, H.-S., Kleinen, T., Krummel, P., Lamarque, J.-F., Langenfelds, R., Locatelli, R., Machida, T., Maksyutov, S., McDonald, K. C., Marshall, J., Melton, J. R., Morino, I., Naik, V., O´Doherty, S., Parmentier, F.-J. W., Patra, P. K., Peng, C., Peng, S., Peters, G. P., Pison, I., Prigent, C., Prinn, R., Ramonet, M., Riley, W. J., Saito, M., Santini, M., Schroeder, R., Simpson, I. J., Spahni, R., Steele, P., Takizawa, A., Thornton, B. F., Tian, H., Tohjima, Y., Viovy, N., Voulgarakis, A., van Weele, M., van der Werf, G. R., Weiss, R., Wiedinmyer, C., Wilton, D. J., Wiltshire, A., Worthy, D., Wunch, D., Xu, X., Yoshida, Y., Zhang, B., Zhang, Z. and Zhu, Q.: The global methane budget 2000–2012, Earth Syst. Sci. Data, 8(2), 697–751, doi:10.5194/essd-8-697-2016, 2016.

Schloss, P. D., Westcott, S. L., Ryabin, T., Hall, J. R., Hartmann, M., Hollister, E. B., Lesniewski, R. A., Oakley, B. B., Parks, D. H., Robinson, C. J., Sahl, J. W., Stres, B., Thallinger, G. G., Van Horn, D. J. and Weber, C. F.: Introducing mothur: Open-Source, Platform-Independent, Community-Supported Software for Describing and Comparing Microbial Communities, Appl. Environ. Microbiol., 75(23), 7537–7541, doi:10.1128/AEM.01541-09, 2009.

Semrau, J. D., DiSpirito, A. A. and Yoon, S.: Methanotrophs and copper, FEMS Microbiol. Rev., 34(4), 496–531, doi:10.1111/j.1574-6976.2010.00212.x, 2010.

Shakhova, N., Semiletov, I., Salyuk, A., Yusupov, V., Kosmach, D. and Gustafsson, Ö.: Extensive methane venting to the atmosphere from sediments of the East Siberian Arctic shelf, Science, 327(5970), 1246–1250, doi:10.1126/science.1182221, 2010.

Steinle, L., Graves, C. A., Treude, T., Ferré, B., Biastoch, A., Bussmann, I., Berndt, C., Krastel, S., James, R. H., Behrens, E., Böning, C. W., Greinert, J., Sapart, C.-J., Scheinert, M., Sommer, S., Lehmann, M. F. and Niemann, H.: Water column methanotrophy controlled by a rapid oceanographic switch, Nat. Geosci., 8(5), 378–382, doi:10.1038/ngeo2420, 2015.

Steinle, L., Schmidt, M., Bryant, L., Haeckel, M., Linke, P., Sommer, S., Zopfi, J., Lehmann, M. F., Treude, T. and Niemannn, H.: Linked sediment and water-column methanotrophy at a man-made gas blowout in the North Sea: Implications for methane budgeting in seasonally stratified shallow seas: Linked sediment and water methanotrophy, Limnol. Oceanogr., 61(S1), S367–S386, doi:10.1002/lno.10388, 2016.

Stoddard, S. F., Smith, B. J., Hein, R., Roller, B. R. K. and Schmidt, T. M.: rrnDB: improved tools for interpreting rRNA gene abundance in bacteria and archaea and a new foundation for future development, Nucleic Acids Res., 43(D1), D593–D598, doi:10.1093/nar/gku1201, 2015.

Strong, P. J., Xie, S. and Clarke, W. P.: Methane as a Resource: Can the Methanotrophs Add Value?, Environ. Sci. Technol., 49(7), 4001–4018, doi:10.1021/es504242n, 2015.

Tanaka, K., Takesue, N., Nishioka, J., Kondo, Y., Ooki, A., Kuma, K., Hirawake, T. and Yamashita, Y.: The conservative behavior of dissolved organic carbon in surface waters of the southern Chukchi Sea, Arctic Ocean, during early summer, Sci. Rep., 6(1), doi:10.1038/srep34123, 2016.

Thomas, D. N. and Dieckmann, G. S.: Antarctic Sea Ice–a Habitat for Extremophiles, Science, 295(5555), 641–644, doi:10.1126/science.1063391, 2002.

Tsunogai, U., Yoshida, N., Ishibashi, J. and Gamo, T.: Carbon isotopic distribution of methane in deep-sea hydrothermal plume, Myojin Knoll Caldera, Izu-Bonin arc: implications for microbial methane oxidation in the oceans and applications to heat flux estimation, Geochim. Cosmochim. Acta, 64(14), 2439–2452, doi:10.1016/S0016-7037(00)00374-4, 2000.

Uhlig, C. and Loose, B.: Using stable isotopes and gas concentrations for independent constraints on microbial methane oxidation at Arctic Ocean temperatures: Methane oxidation rates from stable isotopes, Limnol. Oceanogr. Methods, doi:10.1002/lom3.10199, 2017.

Valentine, D. L., Blanton, D. C., Reeburgh, W. S. and Kastner, M.: Water column methane oxidation adjacent to an area of active hydrate dissociation, Eel river Basin, Geochim. Cosmochim. Acta, 65(16), 2633–2640, doi:10.1016/S0016-7037(01)00625-1, 2001.

Valentine, D. L., Kessler, J. D., Redmond, M. C., Mendes, S. D., Heintz, M. B., Farwell, C., Hu, L., Kinnaman, F. S., Yvon-Lewis, S., Du, M., Chan, E. W., Tigreros, F. G. and Villanueva, C. J.: Propane respiration jump-starts microbial response to a deep oil spill, Science, 330(6001), 208–211, doi:10.1126/science.1196830, 2010.

Verdugo, J., Damm, E., Snoeijs, P., Díez, B. and Farías, L.: Climate relevant trace gases ($N_2O$ and $CH_4$) in the Eurasian Basin (Arctic Ocean), Deep Sea Res. Part Oceanogr. Res. Pap., 117, 84–94, doi:10.1016/j.dsr.2016.08.016, 2016.

Vrede, K., Heldal, M., Norland, S. and Bratbak, G.: Elemental Composition (C, N, P) and Cell Volume of Exponentially Growing and Nutrient-Limited Bacterioplankton, Appl. Environ. Microbiol., 68(6), 2965–2971, doi:10.1128/AEM.68.6.2965-2971.2002, 2002.

Wang, S. W., Budge, S. M., Gradinger, R. R., Iken, K. and Wooller, M. J.: Fatty acid and stable isotope characteristics of sea ice and pelagic particulate organic matter in the Bering Sea: tools for estimating sea ice algal contribution to Arctic food web production, Oecologia, 174(3), 699–712, doi:10.1007/s00442-013-2832-3, 2014.

Whiticar, M. J.: Carbon and hydrogen isotope systematics of bacterial formation and oxidation of methane, Chem. Geol., 161(1–3), 291–314, doi:10.1016/S0009-2541(99)00092-3, 1999.

Yamamoto, S., Alcauskas, J. B. and Crozier, T. E.: Solubility of methane in distilled water and seawater, J. Chem. Eng. Data, 21(1), 78–80, doi:10.1021/je60068a029, 1976.

Zhou, J., Tison, J.-L., Carnat, G., Geilfus, N.-X. and Delille, B.: Physical controls on the storage of methane in landfast sea ice, The Cryosphere, 8(3), 1019–1029, doi:10.5194/tc-8-1019-2014, 2014.

Biogeosciences Discuss., https://doi.org/10.5194/bg-2017-410
Manuscript under review for journal Biogeosciences
Discussion started: 13 October 2017


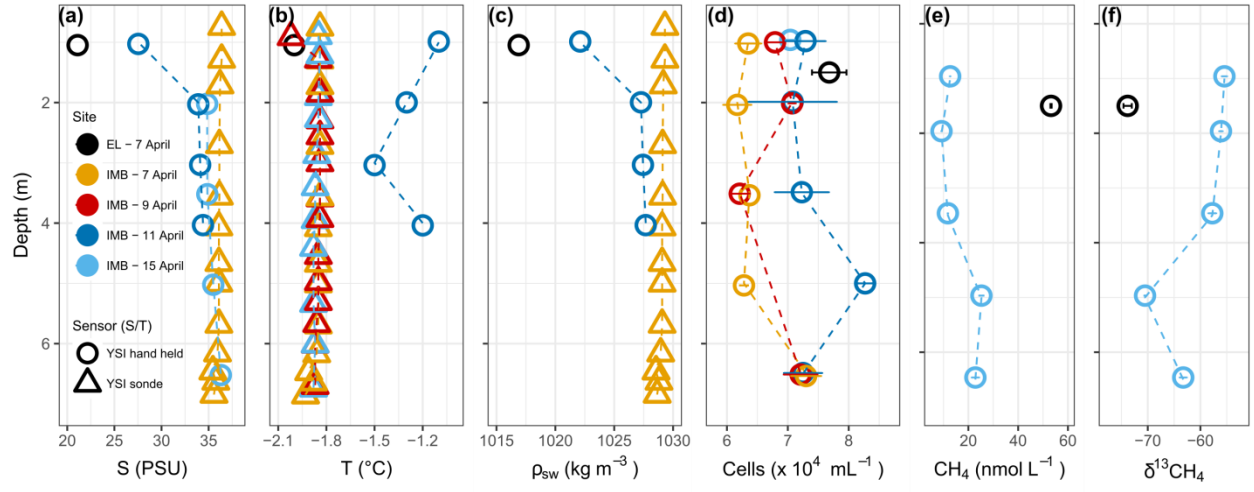


**Figure 1: Water column properties during the time series near Utqiagvik. Salinity (a), temperature (b), density (c), cell numbers (d), methane concentration (a) and stable isotope ratios (b). Error bars on cell numbers (d) is the standard deviation on two technical replicates. Temperature and salinity were determined with an YSI hand held (circle) and YSI sonde (triangle). Salinity for the YSI sonde on 9 and 15 April is missing due to freezing of the sensor. Methane data is only available for EL at 7 April and for IMB at 15 April.**

Biogeosciences Discuss., https://doi.org/10.5194/bg-2017-410
Manuscript under review for journal Biogeosciences
Discussion started: 13 October 2017


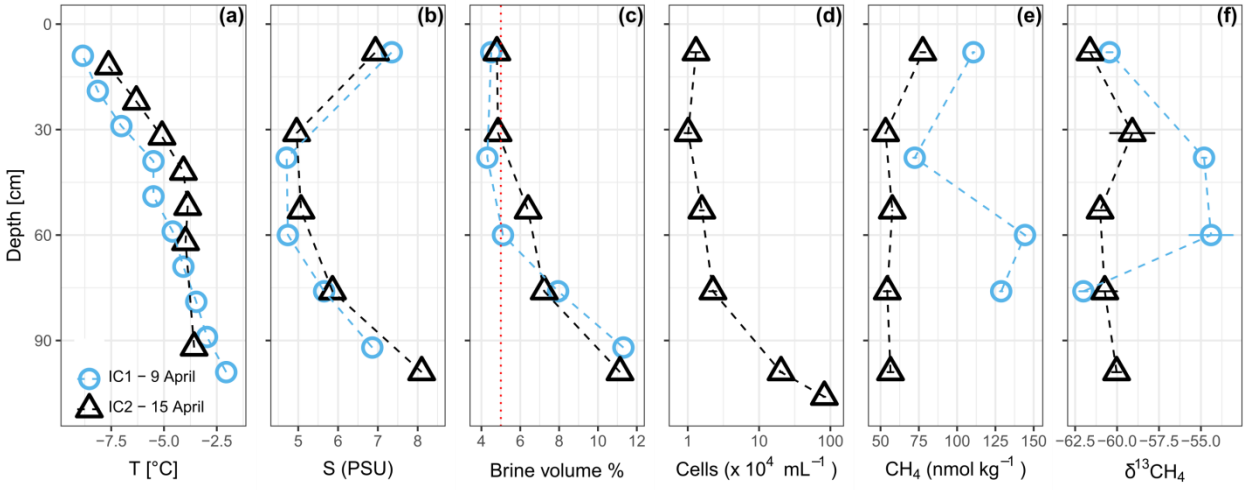


**Figure 2: Sea ice temperature (a), bulk salinity (b), brine volume fraction (c), prokaryotic cells $mL^{-1}$ sea ice (d), methane concentration (e) and stable isotope ratios (f). The vertical red dotted line in (c) shows a brine volume fraction of 5%, the threshold for permeability (Golden et al., 1998). IC1 had sediment included into the ice matrix at depth 30–46 cm, indicated by the gray box.**

Biogeosciences Discuss., https://doi.org/10.5194/bg-2017-410
Manuscript under review for journal Biogeosciences
Discussion started: 13 October 2017


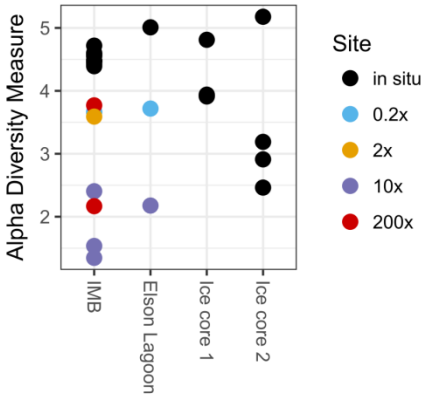


**Figure 3: Shannon indices of alpha diversity for V4V5 amplicons.**

Biogeosciences Discuss., https://doi.org/10.5194/bg-2017-410
Manuscript under review for journal Biogeosciences
Discussion started: 13 October 2017


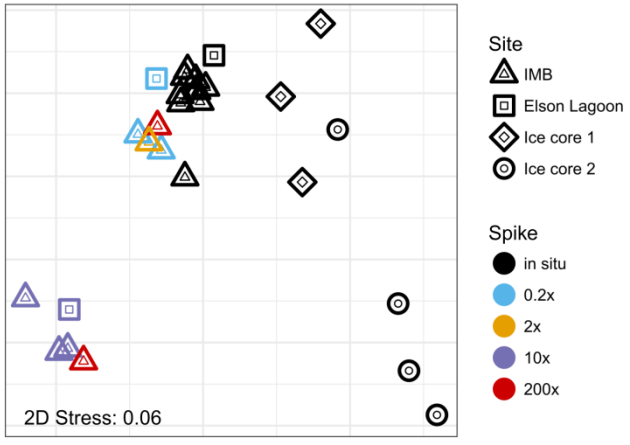


**Figure 4: Non-metric multidimensional scaling analysis (unitless) of Bray-Curtis dissimilarities of the original 16S read data. The low 2D stress of 0.06 indicates a good two-dimensional representation of the multidimensional dataset with very low prospect of misinterpretation.**

Biogeosciences Discuss., https://doi.org/10.5194/bg-2017-410
Manuscript under review for journal Biogeosciences
Discussion started: 13 October 2017


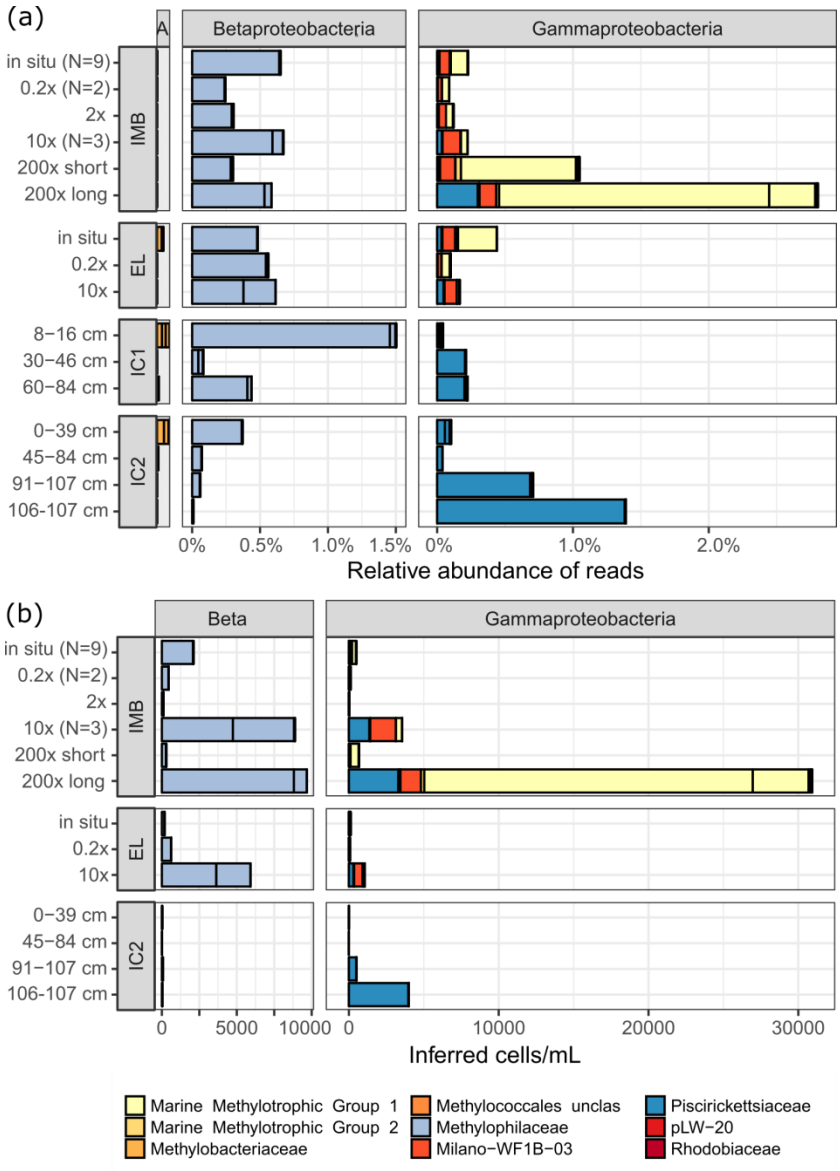


**Figure 5: Relative abundances (a) and inferred cell numbers (b) of methylotroph OTUs by family. Sampling site for water samples are mass balance buoy (IMB) and Elson Lagoon (EL). Ice cores (IC1 and IC2) were collected at site IMB on 9 and 15 April, respectively. The sample name indicates the methane spike concentration compared to in situ methane concentration for IMB and EL, and the ice core section in cm from top (0 cm, ice-snow interface) to bottom (ice-water interface). IMB in situ, 0.2x and 10x are averages of the respective number (N) of samples, all other samples were N=1. Red and yellow shades indicate MOB, while blue shades indicate non-MOB-methylotrophs. (a) α-Proteobacteria (A), β-Proteobacteria (Beta) and γ-Proteobacteria are shown; Verrucomicrobia Incertae Sedis were < 0.003% in (a). Scale for α-Proteobacteria is the same as for β- and γ-Proteobacteria. (b) Cell numbers were calculated from the relative abundances shown in (a) with the cell counts from flow cytometry and corrected for the 16S copy number per cell. Verrucomicrobia Incertae Sedis and α-Proteobacteria were < 8 cells $mL^{-1}$.**

Biogeosciences Discuss., https://doi.org/10.5194/bg-2017-410
Manuscript under review for journal Biogeosciences
Discussion started: 13 October 2017


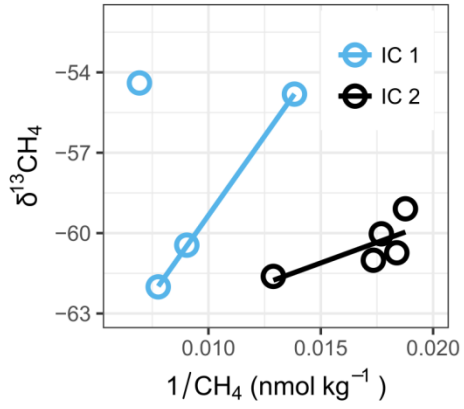


**Figure 6: $\delta^{13}CH_4$ vs. reciprocal of $CH_4$ concentration (Keeling type plot) of ice cores. The correlation between more positive $\delta^{13}CH_4$ and a decrease $CH_4$ concentration in each ice core indicates microbial oxidation. Comparing IC2 to IC1, the shift to higher concentrations and more positive $\delta^{13}CH_4$ (see also Fig. 2) in IC1 might indicate $CH_4$ production from a substrate with heavier isotope signature, compared to the values in IC2.**

Biogeosciences Discuss., https://doi.org/10.5194/bg-2017-410
Manuscript under review for journal Biogeosciences
Discussion started: 13 October 2017


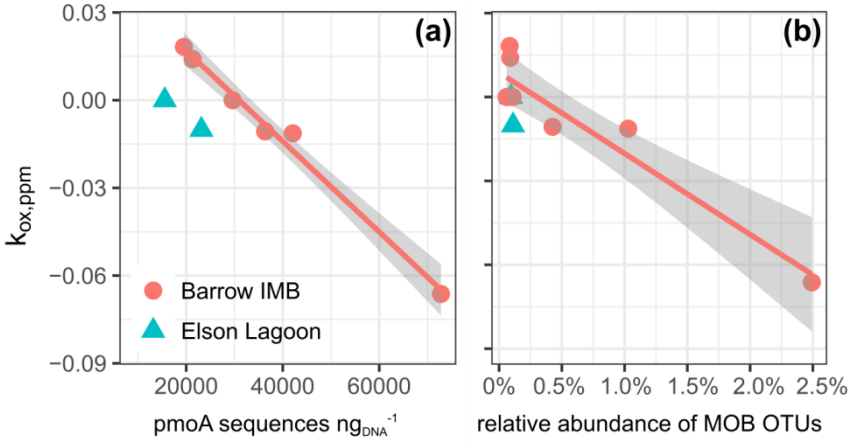


**Figure 7: Correlation between the oxidation rate constant ($k_{ox,ppm}$) and the number of pmoA sequences with $R^2_{(pmoA\sim kox)}$ = 0.85 (a) and the relative number of sequences in ´MOB´-OTUs $k_{ox}$=0.0065 x MOB% - 3.15, $R^2_{(MOB\text{-}OUTs\sim kox)}$ = 0.84 (b). For correlation to the number of total methylotroph OTUs (which includes MOB and non-MOB-methylotrophs) $R^2_{(´Meth´\text{-}OUTs\sim kox)}$ = 0.81. The gray shaded area shows the 95% confidence interval of the correlation.**

Biogeosciences Discuss., https://doi.org/10.5194/bg-2017-410
Manuscript under review for journal Biogeosciences
Discussion started: 13 October 2017


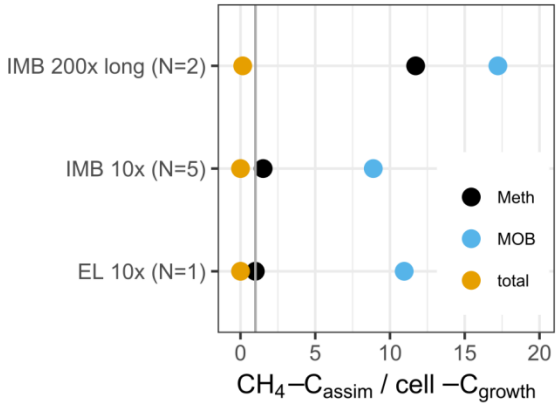


**Figure 8: Ratio of methane-carbon assimilated ($CH_4$-$C_{assim}$) to cell-C gained during growth (cell-$C_{growth}$) based on flow cytometric cell counts (total) or inferred cell numbers (Meth, MOB). The standard deviation between replicates for replicates was 10–20%. The vertical line indicates a ratio of 1. Above 1 the entrie cell gain can be explained by the assimilated $CH_4$.**

Biogeosciences Discuss., https://doi.org/10.5194/bg-2017-410
Manuscript under review for journal Biogeosciences
Discussion started: 13 October 2017


**Table 1: Station and sample list**

| Name[1] | Date | Position | Samples | Parameters[2] |
|---|---|---|---|---|
| EL | 07.04.2016 | 71.334° N, -156.363° W | water | in situ $CH_4$, ox rate, T/S, DNA, cell counts, nutrients |
| IMB 1 | | 71.373° N, -156.548° W | water | ox rate, DNA, cell counts, nutrients |
| IMB 2 | 09.04.2017 | 71.372° N, -156.540° W | water | ox rate, DNA, cell counts, nutrients |
| | | | ice core 1 | in situ $CH_4$, T/S, DNA |
| IMB 3 | 11.04.2015 | 71.372° N, -156.540° W | water | T/S, DNA, nutrients depth profile, cell counts |
| IMB 4 | 15.04.2017 | 71.372° N, -156.540° W | water | in situ $CH_4$ depth profile, DNA |
| | | | ice core 2 | in situ $CH_4$, T/S, DNA |

[1]Station abbreviations are Elson Lagoon (EL) and ice mass balance buoy (IMB)

[2]Paramters: in situ concentration and $\delta^{13}CH_4$ (in situ $CH_4$), oxidation rate (ox rate), temperature and salinity (T/S), collection of biomass for DNA extraction (DNA), cell counts, nutrients

Biogeosciences Discuss., https://doi.org/10.5194/bg-2017-410
Manuscript under review for journal Biogeosciences
Discussion started: 13 October 2017


**Table 2: Samples sequenced for V4V5 and pmoA**

| treatment | site | V4V5 # of samples | pmoA # of samples |
|---|---|---|---|
| in situ | IMB | 9 | 4 |
| | EL | 1 | 1 |
| | sea ice | 7 | 0 |
| 0.2x, 10 days | IMB | 2 | 3 |
| | EL | 1 | 1 |
| 2x, 5 days | IMB | 1 | 1 |
| 10x, 46 days | IMB | 3 | 2 |
| | EL | 1 | 1 |
| 200x, 6 days | IMB | 1 | 1 |
| 200x, 41 days | IMB | 1 | 1 |

Biogeosciences Discuss., https://doi.org/10.5194/bg-2017-410
Manuscript under review for journal Biogeosciences
Discussion started: 13 October 2017


**Table 3: Methane oxidation parameters during long term incubation experiments. N: number of replicates, $k_{ox,ppm}$ : oxidation rate constant, $r_{ox,ppm}$: oxidation rate, $\alpha_{ox}$: isotopic fractionation factor during oxidation. Oxidation rates and rate constants from Uhlig and Loose 2017**

| treatment | N | Incubation [days] | $k_{ox,ppm}$ [$d^{-1}$] | $r_{ox,ppm}$ [nmol $L^{-1}$ $d^{-1}$] | $\alpha_{ox}$ |
|---|---|---|---|---|---|
| 0.2x EL | 1 | 10 | 0[1] | 0[1] | 0.9591 |
| 10x EL | 1 | 46 | $1.01 \times 10^{-2}$ | 0.62 | 1.0230 |
| 0.2x IMB 1 | 5 | 10 | $-1.05 \times 10^{-2}$ | Negative[2] | 0.994 ± 0.0113 |
| 2x IMB 2 | 4 | 5 | 0[1] | 0[1] | 0.9898 ± 0.0104 |
| 10x IMB 1 | 5 | 46 | $9.18 \times 10^{-3}$ | 0.16 ± 0.02 | 1.0225 ± 0.0005 |
| 200x IMB 2 short | 7 | 6 | 0[1] | 0[1] | 1.0005 ± 0.0005 |
| 200x IMB 2 long | 2 | 41 | $6.62 \times 10^{-2}$ | 1.14 ± 0.18 | 1.0103 ± 0.0002 |
| 200x IMB 2 NaOH | 1 | 41 | 0[1] | 0[1] | 0.9998 |

[1]Oxidation rate constants were not significantly different from 0 at a 95% confidence level

[2]Negative oxidation rate constant indicating methane production

Biogeosciences Discuss., https://doi.org/10.5194/bg-2017-410
Manuscript under review for journal Biogeosciences
Discussion started: 13 October 2017


**Table 4: Relative abundance of Methylotroph-OTUs in situ, split into methanotrophs (MOB) and non-MOB-methylotrophs ("Methy")**

| | | in situ sea ice | in situ sea water | 0.2x, 2x (short) | 10x (long) | 200x (long+short) |
|---|---|---|---|---|---|---|
| N | | 7 | 10 | 4 | 4 | 2 |
| Mean ± sd | MOB | 0.04% ± 0.04% | 0.24% ± 0.09% | 0.09% ± 0.01% | 0.17% ± 0.15% | 1.76% ± 0.73% |
| | Methy | 0.74% ± 0.50% | 0.65% ± 0.12% | 0.34% ± 0.13% | 0.70% ± 0.62% | 0.61% ± 0.29% |
| min | MOB | 0.00% | 0.06% | 0.08% | 0.06% | 1.03% |
| | Methy | 0.11% | 0.51% | 0.23% | 0.20% | 0.32% |
| max | MOB | 0.11% | 0.45% | 0.11% | 0.43% | 2.49% |
| | Methy | 1.53% | 0.83% | 0.56% | 1.72% | 0.90% |

Biogeosciences Discuss., https://doi.org/10.5194/bg-2017-410
Manuscript under review for journal Biogeosciences
Discussion started: 13 October 2017


**Table 5: Spearman rank order correlations coefficients ($\rho_S$) of $k_{ox,ppm}$ vs. the number of sequences of pmoA MOB and non-MOB methylotrophs, and candidate OTUs**

| | Total | Normalized[2] | Relative abundance | Inferred cell density[3] |
|---|---|---|---|---|
| pmoA | -0.86**[3] | n.d. | n.d. | n.d. |
| methylotrophs | -0.81** | -0.97*** | -0.79** | -0.63. |
| MOB | -0.82** | -0.66* | -0.82** | -0.61. |
| non-MOB | -0.71* | -0.80** | -0.69* | -0.58. |
| candidate OTUs[4] | -0.07 [ns] | -0.23 [ns] | -0.03[ns] | n.d. |

[1]Levels: $\rho_S < 0.8$ very strong, $0.6 < \rho_S < 0.8$ strong

[2]normalized to total abundance of reads using the DESeq2 package

[3]MOB cell density was calculated from relative abundance and flow cytometry cell counts, weighted for copy number of 16S for respective OTUs

[4]Significance levels: 0 '***' 0.001 '**' 0.01 '*' 0.05 '.' 0.1 'ns ' 1

[5]Candidate OTUs are OTUs that were differentially more abundant in 10x and 200x incubated samples